Department of Physical Science

University of Mumbai - Department of Atomic Energy (**UM-DAE**)

CENTRE FOR EXCELLENCE IN BASIC SCIENCES, MUMBAI

Master's Thesis

of

Ayush Padhan

P0191315, School of Physical Sciences,

titled

THE KRYLOV-WIGNER FUNCTION AND COMPLEXITY GROWTH MINIMIZATION

for the degree of

MASTERS OF PHYSICAL SCIENCE

Submitted on

9th May 2024

Thesis Adviser

Prof. Onkar Parrikar

Professor, Department of Theoretical Physics,

Tata Institute of Fundamental Research, Mumbai

Abstract

The study investigates the discrete Wigner function derived from the Krylov basis in a D-dimensional Hilbert space, building upon the research by O. Parrikar et. al.[3]. By exploring the concept of negativity of the Wigner function and its relation with the case of quantum chaos, particularly in the realm of quantum computation correlations, it demonstrates the Krylov basis's effectiveness in curtailing the initial growth of Wigner negativity, especially in scenarios with large D. Furthermore, the thesis examines the evolution of the Wigner negativity over time, identifying three distinct phases: a gradual increase over $O(\sqrt{D})$ time, followed by a sharp ascent, and eventual stabilization near its upper limit of $\sqrt{D}$. It also presents numerical analysis within the framework of random matrix theory, specifically dealing with the Gaussian Orthogonal Ensemble (GOE), which further strengthens the parent reference results [3]. This study sheds light on the dynamics of the Krylov-Wigner function and its sum negativity. Overall, this study contributes to our understanding of the practicality of the Krylov basis in elucidating chaotic quantum dynamics, with potential implications for the AdS/CFT correspondence.

Acknowledgments

I would like to thank my guide Prof. Onkar Parrikar for his constant support and motivation. I am grateful to him for his continuous help throughout this study and for giving me all the freedom and space, I needed to do the project. I would like to thank my friends especially Aadharsh, Syed, and Aditya Tripathi for their support and help in compiling all the data and formatting the report. I would also like to thank my colleague and mentor in TIFR, Ritam Basu, who was involved in the development of the project, and others who were willing to support me with their skills. I would like to thank my parents and my teachers for their support and blessings. Lastly, I would like to thank the Department of Physical Sciences of UM-DAE-CEBS for providing a much-needed wonderful academic ambiance to successfully carry out this study.

Table of Contents

List of Figures

Chapter 1

Introduction

Quantum systems, with their inherent complexity and non-intuitive behaviours, often defy easy classical descriptions. Yet, understanding whether a quantum system possesses a classical analogue, particularly one conducive to efficient computational analysis, is a fundamental question with wide-ranging implications across various disciplines, from quantum information theory to quantum gravity.

The quest for identifying quantum systems with useful classical descriptions has spurred significant research endeavours. One notable example is the AdS/CFT correspondence, where a classical gravitational theory in anti-de Sitter space (AdS) is conjectured to be dual to a strongly coupled quantum field theory (CFT) living on its boundary. This duality, with the bulk theory's semiclassical description emerging from the boundary quantum system, underscores the intricate interplay between quantum and classical realms. Motivated by such intriguing correspondences, our study delves into the realm of quantum complexity and the quest for classical analogues therein. We draw inspiration from quantum information theory, where the search for efficient classical descriptions of quantum circuits poses analogous questions. Specifically, given a quantum circuit, can it be efficiently simulated by a classical algorithm, thus indicating a useful classical description of the quantum dynamics?

Our investigation focuses on leveraging the concept of the Krylov basis—a powerful tool in both quantum computation and quantum chaos—to probe the relationship between quantum complexity and classical analogues. In the *first chapter*, we delve into the theoretical underpinnings of quantum complexity and its connection to the Krylov basis. We begin by exploring the concept of quantum chaos and spread complexity, elucidating how complexity computations relate to the spread of states in quantum systems. Then, we delve into the realm of random matrix theory (RMT), where we utilize the Lanczos approach to construct the Krylov basis, setting the stage for our subsequent investigations[1]. By studying the statistics of Lanczos coefficients, we gain insights into the nature of quantum complexity and its manifestations in chaotic quantum dynamics.

In the *second chapter*, we thoroughly explore the Wigner function, a potent method for describing quantum states in phase space. We start by understanding how to build the Wigner function using Weyl transforms and then investigate how it changes over time. We also introduce the discrete Wigner function and examine its characteristics in quantum systems[7]. Additionally, we delve into the concept of Wigner negativity, which helps us understand quantum correlations, and analyze its significance in fields like quantum computation and chaos theory.

In the next pivotal *third chapter*, we synthesize the insights gleaned from Chapters 2 and 3 to develop the Krylov-Wigner (KW) function— a novel construct that bridges the gap between quantum complexity and classical analogues, as first developed by my advisor, O. Parrikar and his group in [3]. We lay the groundwork by establishing the theoretical framework for the KW function and delve into its implications for understanding the spread of quantum states in phase space. Through numerical analysis, we study the growth dynamics of KW negativity as well as its relationship to chaotic quantum dynamics and the feasibility of semiclassical descriptions in complex quantum systems.

By amalgamating insights from quantum computation, chaos theory, and quantum gravity, our study contributes to the broader quest for understanding the interplay between quantum complexity and classical analogues. Through this exploration, we aim to unveil the underlying principles guiding the emergence of classical descriptions in complex quantum systems, paving the way for deeper insights into the nature of quantum complexity and its semiclassical manifestations.

Chapter 2

Quantum Complexity and Krylov basis

2.1 Quantum chaos and spread complexity

2.1.1 Spread complexity

Consider a quantum system with a time-dependent Hamiltonian H. Time evolution of a state $|\psi(t)\rangle$ satisfying such a Hamiltonian is given by the Schrodinger equation

$$i\partial_t|\psi(t)\rangle = H|\psi(t)\rangle \tag{2.1}$$

The solution is given by $|\psi(t)\rangle = e^{-iHt}|\psi(0)\rangle$, where $|\psi(0)\rangle$ is the wavefunction at $t = 0$. Using Taylor expansion, we can write the solution as

$$|\psi(t)\rangle = \sum_{n=0}^{\infty} \frac{(-it)^n}{n!}|\psi_n\rangle \tag{2.2}$$

where $|\psi_n\rangle = H^n|\psi_0\rangle$. The set of ψ's form a complete basis for the subset space of Hilbert space spanned by the wavefunction in finite time t. Applying the Gram-Schmidt procedure for this set of bases and defining the first basis vector as $|K_0\rangle \equiv |\psi_0\rangle$, an ordered, orthonormal basis $\mathcal{K}$ is generated for the desired subset of Hilbert space. This set of basis $\mathcal{K}$ is called the Krylov basis. Driven by the speculation that the more the wavefunction spreads with time, the more the spread complexity and size of the subset spanned in Hilbert space, the idea of spread complexity and its quantification is introduced.

1. **Complete Hilbert space basis:** A complete orthonormal, ordered basis spanning the complete Hilbert space is introduced

$$B = \{\, |B_n\rangle : n = 0, 1, 2, \dots \,\} \tag{2.3}$$

2. **Cost function:** A cost function is defined with the help of this complete basis

$$C_B(t) = \sum_n c_n |\langle\psi(t)|B_n\rangle|^2 \equiv \sum_n c_n p_B(n, t) \tag{2.4}$$

where c_n are positive, increasing sequence of real numbers, and p_B is the probability of $\psi(t)$ having a component in some $\langle B_k|$. By definition, $\sum_n p_B(n,t) = 1$ imposes that the more the wavefunction spreads, the more the number of B_n's occupied by the evolved wave function, and the higher the price of the cost function.

3. **Spread complexity:** It is natural to define complexity as the minimum of this cost function over all such bases $\mathcal{B}$.

$$C(t) = \min_{\mathcal{B}} C_{\mathcal{B}}(t)$$

Conventionally, any basis $\mathcal{B}$ with $|B_0\rangle = |\psi(t_0)\rangle$ will minimize at a given time t_0

$$C(t_0) = \sum_n c_n |\langle \psi(t_0)|B_n\rangle|^2 = c_0 |\langle \psi(t_0)|B_0\rangle|^2 = c_0 \tag{2.5}$$

So, a more accurate measure will be to seek for a "functional minimization" which includes information about the spread of the state over a finite amount of time.
Let $C_{\mathcal{B}}^{(m)} \equiv C_{\mathcal{B}}^{(m)}(0) = \frac{\mathrm{d}^m C_{\mathcal{B}}}{\mathrm{d}t^m}|_{t=0}$. It is assumed that the cost functions for the concerned bases have convergent Taylor series over a finite time domain. For two bases $\mathcal{B}_1$ and $\mathcal{B}_2$, the cost function is given by

$$C_{\mathcal{B}_i}(t=0) = C_{\mathcal{B}_i}^{(0)} + C_{\mathcal{B}_i}^{(1)} t + C_{\mathcal{B}_i}^{(2)} t^2 + \dots \tag{2.6}$$

The idea is that there exist a k such that $C_{\mathcal{B}_1}^{(m)} = C_{\mathcal{B}_2}^{(m)}$ for $m < k$ and $C_{\mathcal{B}_1}^{(m)} < C_{\mathcal{B}_2}^{(m)}$ for $m = k$, then it can be said that $C_{\mathcal{B}_1}(t) < C_{\mathcal{B}_2}(t)$ in the finite time domain $0 \le t \le \tau$, for some $\tau < T$. *So, under a reasonable choice of functional minimization, there is an essentially unique basis minimizing across a finite time domain, which can be determined using the above framework.* Since t is essentially positive, the condition can be formalized using only terms of the sequence of derivatives at $t = 0$:

$$S_{\mathcal{B}} = \left(C_{\mathcal{B}}^{(0)}, C_{\mathcal{B}}^{(1)}, C_{\mathcal{B}}^{(2)}, \dots\right) \tag{2.7}$$

which implies that between two bases, $S_{\mathcal{B}_1} < S_{\mathcal{B}_2}$ if there is some k such that $C_{\mathcal{B}_1}^{(m)} = C_{\mathcal{B}_2}^{(m)}$ for $m < k$ and $C_{\mathcal{B}_1}^{(m)} < C_{\mathcal{B}_2}^{(m)}$ for $m = k$.

Complete Krylov Basis: An ordered basis $\mathcal{B}$ is called complete Krylov basis $\mathcal{K}_c$ iff $\langle B_n| = \langle K_n|$ for $n = 0, 1, \dots, k-1$. The dimension of $\mathcal{K}_c$ need not be same as that of $\mathcal{B}$, infact $\dim(\mathcal{K}_c) \le \dim(\mathcal{B})$. It is proved in [2] that a complete Krylov basis is the functional minimization we seek.

Theorem 2.1.1 *For any basis $\mathcal{B}$, $S_{\mathcal{K}} \leq S_{\mathcal{B}}$, with equality only for the complete Krylov bases $\mathcal{B} = \mathcal{K}_c$.*

Proof: This proof is done by induction, by showing that any orthonormal basis $\mathcal{B}$ whose first N elements coincide with Krylov basis $\mathcal{K}_c$ satisfies $S_{\mathcal{B}} \leq S_{\mathcal{B}'}$ for all $\mathcal{B}' \neq \mathcal{K}_c$ upto the first k basis vectors. We will follow this proof as it inspires a later proof done in the section of the Krylov-Wigner function.

1. Setting the first element of $\mathcal{B}$ as $|B_0\rangle = |\psi_0\rangle$, the cost $C^{(0)}_{\mathcal{B}_1} = C_{\mathcal{B}}(0) = \sum_n c_n |\langle\psi(0)|\mathcal{B}_n\rangle|^2 = c_0$, as the whole basis is orthogonalized. For some $\mathcal{B}'$ with $|\psi(0)\rangle$ distributed in more than one component will have a higher cost, as it will have weighted average of $c_{n\geq 0}$, which are by definition larger than c_0.

2. **Step of induction** The time derivatives of cost function is evaluated

$$\begin{aligned} C^{(m)}_{\mathcal{B}}(t) &= \frac{\mathrm{d}^m C_{\mathcal{B}}}{\mathrm{d}t^m} \\ &= \sum_{n=0}^{N} c_n \frac{\mathrm{d}^m |\langle\psi(0)|\mathcal{B}_n\rangle|^2}{\mathrm{d}t^m} \\ &= \sum_{n=0}^{N} c_n p^{(m)}_{\mathcal{B}}(n,0) \end{aligned} \tag{2.8}$$

   where

$$p^{(m)}_{\mathcal{B}}(n,t) = \frac{\mathrm{d}^m p^{(m)}_{\mathcal{B}}(n,t)}{\mathrm{d}t^m} = i^m \sum_{k=0}^{m} (-1)^k \binom{m}{k} \langle\psi(t)| H^{m-k} |B_n\rangle \langle B_n| H^k |\psi(t)\rangle \tag{2.9}$$

Suppose for some N, $|\mathcal{B}_i = \mathcal{K}_i\rangle$ for $i = 0, \ldots, N-1$, then $p^{(m)}_{\mathcal{B}}(n,t) = p^{(m)}_{\mathcal{K}}(n,t)$ for $n < N$. We need the following lemmas to complete the proof:

Lemma 1: Suppose the first N elements $\mathcal{B}$ are the first N elements of $\mathcal{K}$, up to a phase factor. Then $p^{(m)}_{\mathcal{B}}(n,0) = 0$ for $n \geq N, m < 2N$.

Idea behind proof. For $k < N$, $H^k |\psi(0)\rangle$ is a linear combination of $|\mathcal{B}_0\rangle, \ldots, |\mathcal{B}_{N-1}\rangle$. So, the quantities $\langle\mathcal{B}_N|H^k|\psi(0)\rangle$ and $\langle\psi(0)|H^k|\mathcal{B}_N\rangle$ becomes zero, as $|\mathcal{B}_N\rangle$ is orthogonal to all the $\mathcal{B}_k$'s. Now, for $m \leq 2N-1$, either $m-k$ or k is less than N, which makes (2.9) zero from the above speculation.

Lemma 2: Suppose $|B_i\rangle = |K_i\rangle$ for $i = 0, \cdots N-1$, up to phases. Then, $C^{(2N)}_{\mathcal{B}}(0) \geq C^{(2N)}_{\mathcal{K}}(0)$,

with equality when $\mathcal{K}$ contains precisely N vectors, in which case $\mathcal{B}$ is a complete Krylov basis, or when $|B_N\rangle$ also equals $|K_N\rangle$ up to a phase factor.

Idea behind proof. From Lemma 1, it has been already shown that $p_{\mathcal{B}}^{(m)}(n,0) = 0$ when $m \leq 2N-1$, $n \geq N$ for the basis $\mathcal{B}$ whose first N basis vectors coincide with the Krylov basis up to phases. For $m = 2N$, the (2.9) becomes

$$p_{\mathcal{B}}^{(m)}(n,0) = \binom{2N}{N} \langle\psi|H^N|\mathcal{B}_N\rangle \langle\mathcal{B}_N|H^N|\psi\rangle \tag{2.10}$$

The quantity $H^N|\psi(0)\rangle$ can be represented as $H^N|\psi\rangle = |X\rangle + \sum_i^{N-1} c_i|K_i\rangle$, where by definition $|X\rangle \propto |K_N\rangle$. We have

$$p_{\mathcal{B}}^{(m)}(n,0) = \binom{2N}{N} \langle X|\mathcal{B}_n\rangle \langle\mathcal{B}_N|X\rangle \tag{2.11}$$

Since the bases $\mathcal{B}$ is complete, $\sum_n \langle X|\mathcal{B}_n\rangle \langle\mathcal{B}_N|X\rangle = \langle X|X\rangle$. This condition is satisfied only when $|\mathcal{B}_N\rangle \propto |X\rangle$. The cost function for this basis can be compared with the Krylov basis as

$$\begin{aligned} C_{\mathcal{B}}^{(2N)}(0) &= \sum_n c_n p_{\mathcal{B}}^{(2N)}(n,0) \\ &= \sum_{n=0}^{N-1} c_n p_{\mathcal{B}}^{(2N)}(n,0) + \binom{2N}{N} \sum_{n=N}^{D} c_n \langle X|\mathcal{B}_n\rangle \langle\mathcal{B}_N|X\rangle \\ &\geq \sum_{n=0}^{N-1} c_n p_{\mathcal{K}}^{(2N)}(n,0) + \binom{2N}{N} c_N \langle X|X\rangle \\ &\geq C_{\mathcal{K}}^{(2N)} \end{aligned} \tag{2.12}$$

where D is the dimension of the spanned Hilbert space. With these two lemmas, any basis $\mathcal{B}$ which coincides with the Krylov basis $\mathcal{K}$ in the first N basis elements, the first $2N$ derivatives of cost function are the same as those for $\mathcal{K}$ and if $|\mathcal{B}_N\rangle$ is not $|K_N\rangle$ up to phases, then the $2N$th derivative will cost more. Thus, $S_{\mathcal{B}} \geq S_{\mathcal{K}}$, proving the theorem.

Minimization with discrete time evolution

For our objective, the results need to be extended to discrete-time evolution. According to [2], the Krylov basis minimizes the cost function for all times in the case of discrete-time evolution. The discrete time evolution is given by unitary operators, $U_n|\psi(0)\rangle = |\psi_n\rangle$ with $U_0 = 1$. The Krylov basis in this case is defined in a similar basis, by choosing $|K_0\rangle = |\psi(0)\rangle$ and then recursively orthogonalizing every evolved $|\psi_n\rangle$ with all $|K_j\rangle$ for $j < n$. The proof for the cost function minimization for all times follows similar steps to that in the continuous case.

Complexity in terms of entropy We have an alternative definition of entropy [2], where the spread of the wavefunction can be quantified as the exponential of the entropy of probability

distribution of weights in an orthonormal basis $\mathcal{B}$.

$$C_{H_\mathcal{B}} = \exp\{H_\mathcal{B}\} \tag{2.13}$$

where

$$H_\mathcal{B}(t) = -\sum_n p_\mathcal{B}(n,t) \log p_\mathcal{B}(n,t) \tag{2.14}$$

is the Shannon entropy of the basis weight distribution. Here Krylov basis provides the minimum possible dimension of Hilbert space to store probability distribution at some time t.

2.1.2 Complexity computation

The Krylov basis can be computed via the Lanczos algorithm, which includes applying the Gram-Schmidt procedure to the evolved wave function. For $|\psi_n\rangle = H^n |\psi(0)\rangle$, one can generate the Krylov basis $\mathcal{K} = \{ |K_n\rangle : n = 0, 1, \dots \}$ with the following recursion formula:

$$\begin{aligned} |A_{n+1}\rangle &= (H - a_n) |K_n\rangle - b_n |K_{n-1}\rangle \\ |K_n\rangle &= b_n^{-1} |A_n\rangle \end{aligned} \tag{2.15}$$

where the Lanczos coefficient a_n and b_n are given by

$$a_n = \langle K_n|H|K_n\rangle \ , \ b_n = \langle A_n|A_n\rangle^{1/2} \tag{2.16}$$

with $b_0 \equiv 0$ and $|K_0\rangle = |\psi(0)\rangle$ for the initial state. We observe from (2.15) that the Hamiltonian takes the form of a tridiagonal matrix in the Krylov basis. This is called the "Hessenberg form" for finite-dimensional systems.

$$H |K_n\rangle = a_n |K_n\rangle + b_{n+1} |K_{n+1}\rangle + b_n |K_{n-1}\rangle \tag{2.17}$$

Generating Krylov basis

1. **From Hessenberg matrix form:**

   The Lanczos coefficients can be computed by reducing the Hamiltonian matrix into a tridiagonal form (Hessenberg form) using Householder reflections instead of the Gram-Schmidt method. There are two limitations to this method, the first being the initial state typically defined to be $(1, 0, 0, \dots)^T$, which needs to be modified to $|K_0\rangle$. The second limitation comes from the negative values of off-diagonal elements b_n which sometimes arise from these recursions. One needs to take the absolute values of the off-diagonal entries to get the desired Lanczos coefficients.

2. **From survival amplitude:**

A more general method for computing the Lanczos coefficients is devised in [2] which is valid for infinite dimensional systems and the large N limit of finite dimensional systems. Survival amplitude is defined as:

$$S(t) = \langle\psi(t)|\psi(0)\rangle = \langle\psi(0)|e^{-iHt}|\psi(0)\rangle = \psi_0(t)^* \tag{2.18}$$

It is also a moment-generating function for the Hamiltonian. For nth moment

$$\mu_n = \frac{\mathrm{d}^n S(t)}{\mathrm{d}t^n}\bigg|_{t=0} = \langle\psi(0)|\frac{\mathrm{d}^n e^{-iHt}}{\mathrm{d}t^n}|\psi(0)\rangle\bigg|_{t=0} = \langle K_0|(iH)^n|K_0\rangle \tag{2.19}$$

A Krylov basis is defined as a chain with each $|K_n\rangle$ as a node. For an arbitrary state $\psi(t)$ defined $\sum_n d_n |K_n\rangle$, the action of iH is equivalent to the action of chain transition matrix on chain state vector $(d_0, d_1, d_2, \ldots)$, where d_i denotes the weight on i-th node. We assume the initial state vector as $(1, 0, 0, \ldots)$ and iterate the chain n times giving the weight of individual nodes for n-th iterations. From (2.17), one can observe that the updated weights on the nodes are nothing but a combination of Lanczos coefficients. The moment after n iterations $\mu_n = \langle K_0|(iH)^n|K_0\rangle$ will correspond to the weight of $|K_0\rangle$.

The action of iH on a node as well as the evolution of weights on each node forms a Markov chain as shown in Fig (2.1.). In the given representation, j-th vertical column represents the j-th iteration of the transition matrix and the i-th element of j-th vertical column gives the weight on $|K_i\rangle$. The transition weights $w(e)$ of edges e between two adjacent columns represent the action of (iH). Let the weight of the path of connected edges $P = \{ e_1, e_2, \ldots \}$ as the product of the edges forming the path $w(P) = \prod_{e\in P} w(e)$. With weight of first node defined as $w(node_0) = 1$, the weight of some i-th node in j-th column is given as $w(node_{ij}) = \sum^{ij}_{\text{all paths, } n\,=\,0} w(e)$. As shown, the n-th moment is just the weight of the bottom node. For e.g.

$$\begin{aligned} \mu_1 &= \langle K_0|iH|K_0\rangle = ia_0 \\ \mu_2 &= \langle K_0|(iH)^2|K_0\rangle = -a_0^2 - b_1^2 \end{aligned} \tag{2.20}$$

The number of terms signifies the number of paths that can be taken to the k-th bottom node. Suppose that we know the survival amplitude through some other means, which doesn't involve the Lanczos coefficient, the moments $\mu_0, \ldots, \mu_n$ can calculated by taking

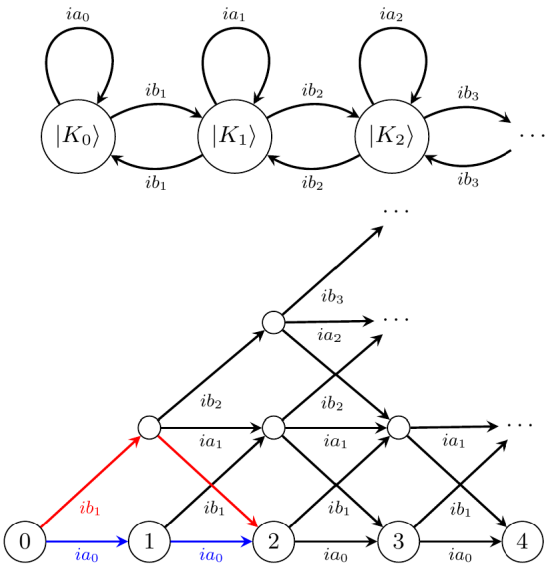

Figure 2.1. Top: "Markov chain" representation of iH. **Bottom**: "*Unwrapping*" of the Markov chain so that "time" goes from left to right. In every vertical column of nodes, the bottom node corresponds to $|K_0\rangle$, the first node above corresponds to $|K_1\rangle$ and so on.

Cited from: *V. Balasubramanium et. al., Quantum chaos and the complexity of spread of states*[2]

derivatives of $S(t)$. The Lanczos coefficients can then be calculated from the moments themselves.

From Fig (2.2.), it can be observed that between adjacent rows (ith - $(i+1)$th), the ascending and descending edges have weight ib_{i+1}, whereas the edges connecting nodes on ith row have weights ia_i and the edges connecting nodes on $(i+1)$th row have weights ia_{i+1}. So, to reach an **odd** bottom node $(2k+1)$, one requires $(2k+1)$ edges. The moment, μ_{2k+1}, is given by the sum of contributions from all the possible paths. From the above discussion, it is observed that only one path includes the contribution from a_k term as seen in Fig 2. The rest of the paths can be calculated using the contributions from $a_0, a_1, \ldots, a_{k-1}$ and $b_1, b_2, \ldots, b_k$. The contribution from a_k term can now be determined.

$$\begin{aligned} \text{Contribution}_{a_k} &= \mu_{2k+1} - \sum_{\text{all other paths}} = X \\ i^{2k+1} b_1^2 b_2^2 \ldots b_k^2 a_k &= X \\ a_k &= \frac{-iX}{b_1^2 b_2^2 \ldots b_k^2} \end{aligned} \tag{2.21}$$

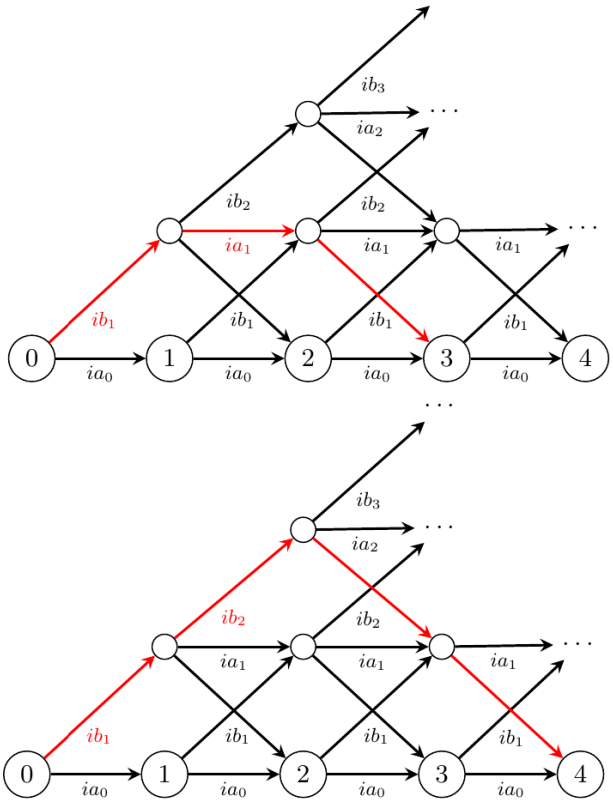

Figure 2.2. Top: Except for the path in red, the weights of every path from node 0 to node 3 can be computed with knowledge just of a_0 and b_1. The weight of the red path can be computed by subtracting the weights of every other path from μ_3, and can then be used to compute a_1. **Bottom**: Except for the path in red, the weights of every path from node 0 to node 4 can be computed with knowledge just of a_0, a_1, and b_1. The weight of the red path can be computed by subtracting the weights of every other path from μ_4, and can then be used to compute b_2.
Cited from: *V. Balasubramanium et. al., Quantum chaos and the complexity of spread of states*[2]

The sum over other paths can be calculated given the values of b_k's and previous a_k's are known. Similarly for **even** moments μ_{2k}, only one path has the contribution from b_k, which goes through an edge of weight ib_k, with a weight $b_1^2 b_2^2 \dots b_k^2$. The weight of all other paths can be computed using only $a_0, \dots, a_k$ and $b_1, \dots, b_{k-1}$. Thus, we can calculate b_k:

$$\begin{aligned} \text{Contribution}_{b_k} &= \mu_{2k} - \sum_{\text{all other paths}} = Y \\ i^{2k} b_1^2 \dots b_{k-1}^2 b_k^2 &= Y \\ b_k^2 &= \frac{-Y}{b_1^2 b_2^2 \dots b_{k-1}^2} \end{aligned} \tag{2.22}$$

Therefore, by employing the recursive algorithm outlined above and ensuring accuracy in computations to handle rounding errors, one can systematically calculate all Lanczos coefficients, starting from the initial Lanczos coefficient, a_0, and the survival amplitude.

Spread Complexity Computation

Once the algorithm for computing the Krylov basis $\mathcal{K}$ and the associated Lanczos coefficient from the survival amplitude is established, the spread complexity of a time-evolving state can be calculated. The Krylov basis must be expanded in terms of itself as $|\psi(t)\rangle = \sum_n \psi_n(t)\,|K_n\rangle$, where unitarity requires $\sum_n |\psi_n(t)|^2 = 1$. Utilizing the Schrödinger equation and (2.17), one obtains

$$i\partial_t \psi_n(t) = a_n \psi_n(t) + b_{n+1}\psi_{n+1}(t) + b_n \psi_{n-1}(t) \tag{2.23}$$

The survival amplitude is the complex conjugate of $\psi_0(t)$. Given $\psi_0(t) = S(t)^*$ and the Lanczos coefficients, one can theoretically compute all the $\psi_n(t)$ using the algebraic procedure defined in the previous section. With $b_0 = 0$, $\psi_0(t)$ and its time derivative in (2.23) can be used to compute $\psi_1(t)$ and subsequently $\psi_2(t)$, and so forth, using the latest $\psi_k(t)$. Given $\psi_n(t)$, the definition of spread complexity allows computation of

$$C(t) = C_{\mathcal{K}}(t) = \sum_n c_n p_n(t) = \sum_n n|\psi_n(t)|^2 \tag{2.24}$$

where the coefficients c_n are $c_n = n$. This quantity can formally be defined as the expectation value in the evolving state $|\psi(t)\rangle$ of the "complexity operator"

$$\hat{K}_\psi = \sum_n n\,|K_n\rangle\,\langle K_n| \tag{2.25}$$

The spread complexity then becomes

$$C(t) = \langle\psi(t)|\hat{K}_\psi|\psi(t)\rangle \tag{2.26}$$

One can also consider the entropic definition of complexity:

$$C_H = e^H = \exp\left\{-\sum_n p_n log p_n\right\} \tag{2.27}$$

where the probability $p_n = |\psi_n|^2$.

Effect of temperature and Thermo-Field Double (TFD) states

To study the growth of spread complexity under the effect of temperature, it is helpful to study the Thermo-Field Double (TFD). It is used to describe systems in thermal equilibrium, especially

when studying thermal properties of quantum systems, Hawking radiation of black holes, and so on. Consider a Hamiltonian H acting on a Hilbert space $\mathcal{H}$ having eigenstates $|n\rangle$ with eigenvalues E_n. We construct the appropriate TFD state as follows:

1. **Doubling the Hilbert space:** A new degree of freedom *(dof)* associated with a second identical copy of Hilbert space $\tilde{\mathcal{H}}$ is introduced. Doubled Hilbert space is spanned by states $|n\rangle \otimes |m\rangle$.

2. **Defining normalized TFD state:** $|\Omega\rangle$ is defined as a superposition of all possible states in doubled Hilbert space, where it is normalized with the partition function

$$|\Omega\rangle = \frac{1}{Z_\beta} \sum_n e^{-\beta E_n/2} |n\rangle \otimes |m\rangle \tag{2.28}$$

3. **Maximally entangled TFD state:** A maximally entangled TFD state is a particular instance of a TFD state where the two subsystems are maximally entangled. In other words, the entanglement between the two subsystems is at its maximum possible value.

$$|\psi_\beta\rangle = \frac{1}{\sqrt{Z_\beta}} \sum_n e^{-\beta E_n/2} |n, n\rangle \tag{2.29}$$

This state is invariant under evolution with Hamiltonian $H_L - H_R$ ($H_{L,R} = H$ act independently on the two copies of $\mathcal{H}$) and not invariant under evolution by the action of just H. Thus, unitary evolution gives:

$$|\psi_\beta(t)\rangle = e^{-iHt} |\psi_\beta\rangle = |\psi_{\beta+2it}\rangle \tag{2.30}$$

The TFD state and its evolution span the subspace defined by $|n, n\rangle$, which results in the finite-dimensional algorithm for the computation of Lanczos coefficients within this subspace. The survival amplitude for the time-evolved TFD state is given by:

$$S(t) = \langle \psi_{\beta+2it} | \psi_\beta \rangle = \frac{Z_{\beta-it}}{Z_\beta} \tag{2.31}$$

where $Z_{\beta-it} = \sum_n e^{-(\beta-it)E_n}$ is the analytically continued partition function. This quantity can be utilized to calculate the spectral form factor (SFF) defined by

$$SFF_{\beta-it} \equiv \frac{|Z_{\beta-it}|^2}{|Z_\beta|^2} \tag{2.32}$$

This is a time-dependent quantity that is extensively studied to understand the chaotic behaviour of a system. In certain universality classes like the Gaussian Unitary Ensemble, the spectral form

factor exhibits universal behaviour independent of the microscopic details of the system and depends only on the global symmetries. It is also interesting to note that SFF measurements can be performed experimentally in various physical systems, e.g. quantum dots, ultracold atomic systems, etc, which can be compared with theoretical predictions.

2.2 Random Matrix Theory (RMT)

A fundamental hypothesis suggests that the intricate characteristics of a quantum chaotic Hamiltonian's spectrum closely resemble the statistical properties of random matrices [2]. This notion suggests that the fine-grained structure of the spectrum of quantum chaos can be effectively approximated by the behaviours observed in randomly generated matrices. Moreover, in light of the energy-time uncertainty principle, it is anticipated that certain dynamics over extended periods in chaotic systems can be adequately captured by examining the statistical distribution of nearby energy eigenvalues within the context of random matrix theory. A good example is in studies focusing on the spectral form factor of the SYK (Sachdev-Ye-Kitaev) model, where the alignment between the model's behaviour and random matrix statistics underscores the broader applicability of this theoretical framework.

There are three universality classes of ensembles:

- **Gaussian Unitary Ensemble (GUE):** Ensemble of of Hermitian $N \times N$ matrices H_{ij} with measure $\frac{1}{Z_{GUE}} e^{-\frac{N}{2}\,\mathrm{Tr}\{H^2\}}$, where $Z_{\mathrm{GUE}} = 2^{N/2}\pi^{N^2/2}$, is the normalizing the partition function.
- **Gaussian Orthogonal Ensemble (GOE):** It is defined as an ensemble of real symmetric $N \times N$ matrices H with measure $\frac{1}{Z_{\mathrm{GOE}}} e^{-\frac{N}{4}\mathrm{Tr}(H^2)}$.
- **Gaussian Symplectic Ensemble (GSE):** It is defined as an ensemble of $N \times N$ Hermitian quaternionic matrices with measure $\frac{1}{Z_{\mathrm{GSE}}} e^{-N\mathrm{Tr}(H^2)}$.

Dyson index can conveniently represent these ensembles: $\beta = 1$ for GOE, $\beta = 2$ for GUE, and $\beta = 4$ for GSE. We can consider a more general case by modifying the measure ($\mathrm{Tr}\{H^2\} \to V(H)$) in the same ensembles. If the potential is invariant under unitary transformation $H \to U\,H\,U^\dagger$, one can further simplify the problem by diagonalizing the matrix. Let U be the unitary diagonalizing matrix and Λ be a diagonal matrix containing eigenvalues, then for a Gaussian

ensemble, one obtains a joint probability distribution of eigenvalues

$$p(\lambda_1, \cdots, \lambda_n) = Z_{\beta,N}\, e^{-\frac{\beta N}{4}\sum_k \lambda_k^2} \prod_{i<j} |\lambda_i - \lambda_j|^\beta \,, \tag{2.33}$$

where $Z_{\beta,N}$ is normalization partition function. For different ensembles, one needs to compute the Jacobian, which gives rise to the Vandermonde determinant $\Delta \equiv \prod_{i<j} |\lambda_i - \lambda_j|^\beta$. Once the distribution is obtained, we can start analyzing the spectrum. The density for eigenvalues of a single matrix is given by

$$\rho(E) = \frac{1}{N}\sum_i \delta(E - \lambda_i) \tag{2.34}$$

where λ_i are the eigenvalues. Since this density depends on random eigenvalues, it would be more appropriate to look at the correlation functions

$$\overline{\rho(E_1)\,\rho(E_1)\,\cdots\,\rho(E_n)}\,. \tag{2.35}$$

One can also compute the partition function, which is just the Laplace transform of the eigenvalue density function

$$Z_\beta = \int_0^\infty dE\,\rho(E)\,e^{-\beta E} \tag{2.36}$$

and also the associated correlation function

$$\overline{Z_{\beta_1}\,Z_{\beta_2}\,\cdots\,Z_{\beta_n}} \tag{2.37}$$

2.2.1 Using Lanczos approach: Krylov basis

Given the time evolution of a state $|\psi(t)\rangle$ is determined by the Schrödinger equation

$$i\partial_t\,|\psi(t)\rangle = H\,|\psi(t)\rangle \tag{2.38}$$

where H is the Hamiltonian, whose entries are obtained from the ensembles discussed above. Using the procedure described in (2.1.1) and (2.1.2), we can obtain the Krylov basis $\mathcal{K}$ via the Lanczos algorithm. Starting from $|\psi_n\rangle = H^n\,|\psi(0)\rangle$, this algorithm generates the orthonormal Krylov basis $\mathcal{K} = \{\,|K_n\rangle : n = 0, 1, 2, \dots\}$ where $|K_n\rangle$ is defined by (2.15) and the Lanczos coefficients a_n and b_n are defined by (2.16).

The resulting Hamiltonian is a tri-diagonal matrix in the Krylov basis, called the "Hessenberg

form" for finite dimensional systems:

$$H = \begin{pmatrix} a_0 & b_1 & & & & \\ b_1 & a_1 & b_2 & & & \\ & b_2 & a_2 & b_3 & & \\ & & \ddots & \ddots & \ddots & \\ & & & b_{N-2} & a_{N-2} & b_{N-1} \\ & & & & b_{N-1} & a_{N-1} \end{pmatrix}. \tag{2.39}$$

For infinite dimensional systems, one can follow a more general method for computing the Lanczos coefficients. It starts from the "survival amplitude" and calculates the Lanczos coefficients from the moments determined using the time derivatives of survival amplitude. Once the Hamiltonian is in tridiagonal form, one can solve the eigenvector-eigenvalue problem without diagonalizing the Hamiltonian further, i.e., without finding the actual eigenvalue/vectors.

Thus, the time evolution becomes a one-dimensional motion with a tridiagonal Hamiltonian. The cost complexity can be calculated from the standard definition as well as the entropic definition of complexity.

2.2.2 Tridiagonalizing random matrices

Problem statement: *Given a Hamiltonian operator in the Hilbert space and a quantum state, one can apply the Lanczos method to obtain a tridiagonal matrix. In RMT we have an ensemble of Hamiltonian, which in turn produces an ensemble of tridiagonal random matrices. The goal is to find the statistics of these matrix elements, the Lanczos coefficient* a_n *and* b_n *given some potential* $V(H)$ *or associated average density of states* $\overline{\rho(E)}$.

The following section identifies the joint distribution of Lanczos coefficients for Gaussian theories and gives the average Lanczos coefficients in a generic RMT.

The Gaussian ensembles

Let's begin with the Gaussian Orthogonal Ensemble (GOE), which is a Gaussian distributed ensemble of orthogonal matrices:

$$\frac{1}{Z_{\text{GOE}}} e^{-\frac{N}{4}\operatorname{Tr}\{H^2\}} \tag{2.40}$$

The initial state is as usual chosen as $|\psi\rangle = (1, 0, 0, \ldots, 0)^T$. The coefficients are in such a basis in which the Hamiltonian is a random matrix drawn from a GOE distribution. Since, the initial

state is always chosen as $|K_0\rangle = |\psi(0)\rangle$, the Lanczos procedure is solved if one finds a similarity transformation O such that

$$OHO^T = \text{Tridiagonal}\ , O\,|\psi(0)\rangle = |\psi(0)\rangle \tag{2.41}$$

where the tridiagonal matrix has real entries and off-diagonal positive entries. Since we need the off-diagonal entries to be positive, the coefficients b_n are subjected to positive real value by choosing phases in the Krylov basis. From (2.41), one observes that the initial state is part of both the initial and transformed bases. Similarity transformation takes the orthonormal basis to some new orthonormal basis, which with the previous observation implies that the new basis obtained from this transformation is the Krylov basis.

We can determine the form of the similarity transformation O. Starting from the second relation of (2.41), the matrix O takes the form

$$O = \begin{pmatrix} 1 & 0 \\ 0 & M \end{pmatrix}\ , \tag{2.42}$$

where $\mathbf{0}$ represent $N-1$ dimensional vectors and M is an $(N-1)\times(N-1)$ matrix. As shown in [1], the following procedure can achieve the tridiagonal form. The Hamiltonian matrix H_N is an $N \times N$ matrix from the GOE ensemble, with the similarity transformation O given by (2.42). The Hamiltonian H_N is of form

$$H_N = \begin{pmatrix} a_0 & x^T \\ x & H_{N-1} \end{pmatrix}\ , \tag{2.43}$$

where $x = (x_1, \ldots, x_{N-1})$ is a $(N-1)$ dimensional vector whose entries are from generic GOE, a_0 is the first entry which denotes the first Lanczos coefficient because of the initial state being part of both the bases, i.e., $a_0 = \langle\psi|H_N|\psi\rangle$. The similarity transformation required to achieve the tridiagonal form has the form

$$OH_NO^T = \begin{pmatrix} a_0 & Mx \\ Mx^T & MH_{N-1}M^T \end{pmatrix} \tag{2.44}$$

The $(N-1)\times(N-1)$ matrix M transforms the generic vector x such that it gets transformed into vector proportional to $e_1 : (1, 0, \ldots)^T$.

$$Mx = \|x\|_2(1, 0, \ldots, 0)^T \equiv \|x\|_2 e_1^T \tag{2.45}$$

where can be stated that $\|x\|_2 = b_1$. This then transform (2.44) into the following form

$$OH_N O^T = \begin{pmatrix} a_0 & \|x\|_2 e_1 \\ \|x\|_2 e_1^T & MH_{N-1}M^T \end{pmatrix} \tag{2.46}$$

It is observed that the statistics of a_0, $\|x\|_2$, and MH_NM^T are uncorrelated due to the statistical relation of GOE [1]. The probability distribution of GOE is proportional to $\exp\left(-N/4\,\mathrm{Tr}\{H^2\}\right)$ with symmetric, Hermitian H, thus each of the entries of H are independently Gaussian up to the symmetricity constraint. The first entry a_0 is invariant under the transformation, whereas the other entries of the first row and column containing $\|x\|_2 e_1$ transforms such that the norm $\|x\|_2$ is the square root of sum of uncorrelated Gaussian random variables with zero mean and variance equal to the off-diagonal entries of the GOE, which produces a χ-distribution.

Now, the $(N-1)\times(N-1)$ matrix H_N is again a random matrix from the GOE ensemble. As all of our transformations are essentially orthogonal transformations (rotations), $MH_{N-1}M^T$ is a random matrix that has GOE ensemble properties. Now taking this as our initial matrix, we repeat the above steps along the diagonal direction, producing a $(N-2)\times(N-2)$ matrix H_{N-2}. This new matrix following the GOE ensemble statistics can again be used as an input matrix and repeat the above procedure until we have tridiagonalized the whole matrix. The variance of the off-diagonal elements is by definition $\chi(N-f)/\sqrt{N}$. Thus the Hamiltonian matrix is transformed as

$$H_N = \begin{pmatrix} a_0 & b_1 & & & \\ b_1 & a_1 & b_2 & & \\ & \ddots & \ddots & \ddots & \\ & & b_{N-2} & a_{N-2} & b_{N-1} \\ & & & b_{N-1} & a_{N-1} \end{pmatrix} = \frac{1}{\sqrt{N}} \begin{pmatrix} N(0,2) & \chi_{(N-1)} & & & \\ \chi_{(N-1)} & N(0,2) & \chi_{(N-2)} & & \\ & \ddots & \ddots & \ddots & \\ & & \chi_2 & N(0,2) & \chi_1 \\ & & & \chi_1 & N(0,2) \end{pmatrix} \tag{2.47}$$

For GUE and GSE, the Lanczos algorithm give rise to the following Lanczos coefficient

$$H_N = \begin{pmatrix} a_0 & b_1 & & & \\ b_1 & a_1 & b_2 & & \\ & \ddots & \ddots & \ddots & \\ & & b_{N-2} & a_{N-2} & b_{N-1} \\ & & & b_{N-1} & a_{N-1} \end{pmatrix} = \frac{1}{\sqrt{\beta\, N}} \begin{pmatrix} N(0,2) & \chi_{(N-1)\beta} & & & \\ \chi_{(N-1)\beta} & N(0,2) & \chi_{(N-2)\beta} & & \\ & \ddots & \ddots & \ddots & \\ & & \chi_{2\beta} & N(0,2) & \chi_\beta \\ & & & \chi_\beta & N(0,2) \end{pmatrix} \tag{2.48}$$

For GOE, GUE, and GSE, it is concluded that the Lanczos coefficients a_n are independent random variables with zero mean and variance equivalent to the ensemble they are derived from. The second set of Lanczos coefficients b_n's, or more appropriately b_n^2's are a chi-squared distribution with $(N-n)\beta$ degrees of freedom whose probability distribution function (pdf) takes the standard form of chi-distribution for b_n's. For a standard chi-squared distribution with n degrees of freedom, the pdf is given by

$$p(x|n) = \frac{1}{\Gamma(n/2)2^{n/2}} x^{\frac{n}{2}-1} e^{-\frac{x}{2}} \ , \ x \in (0,\infty) \tag{2.49}$$

where x is the chi-squared distribution with n degrees of freedom. So, for b_n's, the pdf is given by

$$p(b_n) = 2\left(\frac{\beta N}{2}\right)^{(N-n)\beta/2} \frac{1}{\Gamma((N-n)\beta/2)} b_n^{(N-n)\beta-1} e^{-\beta N b_n^2/2} \tag{2.50}$$

The mean of Lanczos coefficients b_n, $\overline{b_n}$ is

$$\overline{b_n} = \sqrt{\frac{2}{\beta N}} \frac{\Gamma((1+(N-n)\beta)/2)}{\Gamma((N-n)\beta/2)} \tag{2.51}$$

and the variance is of the form

$$\sigma^2 = \overline{(b_n - \overline{b_n})^2} = \frac{(N-n)}{N} - \overline{b_n}^2 \tag{2.52}$$

A nice trick for computing average Lanczos coefficients

For generic RMT with generic densities of states $\rho(E)$, one can generalize the above results to get the statistics of Lanczos coefficients. It is observed that in the case of exact solutions of the Gaussian case, the Lanczos coefficients a_n, b_n have a continuous large-N limit $a(x), b(x)$, when expressed as a function of $x = n/N$ (N being the dimension of Hilbert space) [2]. Assuming this, one can derive an approximate analytical formula relating the density of states to average Lanczos coefficients.

Let H be the Hamiltonian for our system, with Lanczos coefficients a_n, b_n. From (2.23), it is observed that in Krylov basis, the system dynamics simplifies to that of a 1-D chain. The idea is to cut this 1-D Krylov chain into numerous shorter segments (e.g. $\sqrt{N}$ segments of length $\sqrt{N}$), set the $b_n \to 0$ at boundaries of each segment, and take the average of Lanczos coefficients $\overline{a_n}$ and $\overline{b_n}$ for each segment. The claim is that "*For large dimension N, this process approximately preserves the density of states*".

The length of the Krylov chain is the dimension N. Let's define a variable $x = n/N$, where

$0 \leq x \leq 1$ is $N \to \infty$. As $N \to \infty$, $\frac{L}{N} \to 0$, where L is the length of individual segments. Therefore, we have a block approximation of the Hamiltonian, where the density of states is the sum of the densities of these individual segments. The Hamiltonian for each segment, having averaged Lanczos coefficients, has the form of a Toeplitz matrix. A Toeplitz matrix has a tridiagonal form such that the off-diagonal elements both above and below are the same, $T(a,b) = a\mathbf{I} + b\hat{\mathbf{T}}(0,1)$. Here, $\mathbf{T}(0,1)$ is given by a tridiagonal Toeplitz matrix whose diagonal terms are 0 and the off-diagonal terms are 1. The eigenvalues are easier to figure out and are of the form $E_k = a + 2b\cos(k\pi/(L+1))$ with $k = 1, 2, \ldots, L$ and a and b being real and positive. The density of states for such a segment is given by

$$\rho_{a,b}(E) = \frac{1/L}{|dE_k/dk|} = \frac{H(4b^2 - (E-a)^2)}{\pi\sqrt{4b^2 - (E-a)^2}} \tag{2.53}$$

where $H(x)$ is the Heaviside step function so that the density of states is zero outside the interested segment. Therefore, the total density of states is the sum of all the smaller segments, approximated by the integral

$$\rho(E) = \frac{1}{N}\sum_{n=1}^{S} \frac{L\,H(4\,b(nL)^2 - (E-a(nL))^2)}{\pi\sqrt{4\,b(nL)^2 - (E-a(nL))^2}} = \int_0^1 dx\, \frac{H(4\,b(x)^2 - (E-a(x))^2)}{\pi\sqrt{4\,b(x)^2 - (E-a(x))^2}}\,. \tag{2.54}$$

where the average Lanczos coefficients $a(x), b(x)$ are related directly to the density of states.

Consider the n-th order of our tridiagonal Hamiltonian H^n for a more mathematical treatment. Let $[H^n]_{ij}$ be $(i,j)^{\text{th}}$ index entry which is n-th order polynomial of some a_j, b_j with $|j-i| < n$. Let k be an index with n of i, j and let n scale sub-linearly in N in the large N limit so that the difference in x satisfies $|i-k|/N < n/N \to 0$. It can be observed that H^k has two off-diagonal more than H^{k-1}. Thus, H^k can be represented as $H^k = PT(a_k, b_k)^k P^{-1}$, where P is some transformation similar to similarity transformation and a_k, b_k are approximated values for a_i, b_i for large N limit. It is claimed in [2] that $[H^n]_{ij}$ can approximated as

$$[H^n]_{ij} \approx [T(a_k, b_k)^n]_{ij} \tag{2.55}$$

where $T(a,b)$ is an infinite tridiagonal matrix with constant diagonal a and off-diagonal b. It is important to note that although H^n is a finite-dimensional matrix, its elements can be approximated quite accurately by an infinite-dimensional matrix. This doesn't violate anything or make the Hamiltonian H^n infinite-dimensional, it just asserts approximate equality of the elements. Thus, the trace of the moment of H is

$$\text{tr}\{H^n\} = \sum_i [H^n]_{ii} \approx \sum_i [T(a_i, b_i)^n]_{ii} \tag{2.56}$$

We make an approximation with a different matrix for every index i on the left-hand side. These sums can give the following quantities, as shown in [1],

$$[T(a_i, b_i)^n]_{ii} = \int_{a_i-2b_i}^{a_i+2b_i} dE \, \frac{E^n}{\pi\sqrt{4b_i^2 - (E-a_i)^2}} \tag{2.57}$$

$$[T(a_i, b_i)^n]_{i,i+1} = \int_{a_i-2b_i}^{a_i+2b_i} dE \, \frac{E^n(E-a_i)}{b_i\pi\sqrt{4b_i^2 - (E-a_i)^2}} \tag{2.58}$$

where $E = bx + a$. The equation (2.56) is then given by

$$\mathrm{Tr}[H^n] = \int dE\, E^n \rho(E) \approx \frac{1}{N}\sum_i \int_{a_i-2b_i}^{a_i+2b_i} dE \, \frac{E^n}{\pi\sqrt{4b_i^2 - (E-a_i)^2}} \tag{2.59}$$

$$\approx \int_0^1 dx \int_{a(x)-2b(x)}^{a(x)+2b(x)} dE \, \frac{E^n}{\pi\sqrt{4b(x)^2 - (E-a(x))^2}} \tag{2.60}$$

where the sum is converted to an integral for large-N limit and the continuous definitions for $a(x)$ and $b(x)$ are utilized. $\rho(E)$ is normalized so that the integral is one. Using the fact that the polynomials form a complete basis of functions and (2.59), it is observed that $\rho(E)$ is of the form

$$\rho(E) \approx \int_0^1 dx \, \frac{H(4\,b(x)^2 - (E-a(x))^2)}{\pi\sqrt{4\,b(x)^2 - (E-a(x))^2}} \tag{2.61}$$

where $H(t)$ is Heaviside function of t, as $\rho(E)$ exists only between $a(x)-2b(x) \le E \le a(x)+2b(x)$.

Solution to the integral equation The interval of support in E in (2.61) is a function of x, $a(x) - 2b(x) \le E \le a(x) + 2b(x)$. It is known that the outer envelope of the Lanczos coefficients does contract monotonically as mentioned in [1]. It is assumed that "*interval of support in E of integrated of $\rho(E)$ shrinks monotonically as x increases*", i.e., for $x_1 > x_2$,

$$\begin{aligned} a(x_1) + 2b_1(x) &< a(x_2) + 2b_2(x) \\ a(x_1) - 2b_1(x) &> a(x_2) + 2b_2(x) \end{aligned} \tag{2.62}$$

which gives $a'(x) + 2b'(x) < 0$ and $a'(x) - 2b'(x) > 0$ for large values of x. Also, $2b'(x) \le a'(x) < -2b'(x)$ leads to the constraints $b'(x) < 0$ and $|a'(x)| < -2b'(x)$. Starting with $a(x) = 0$, (2.61) becomes even in E with the converse also being true.

$$\rho(E) \approx \int_0^1 dx \frac{H(4b(x)^2 - E^2)}{\pi\sqrt{4b(x)^2 - E^2}} = \int_{b_0}^0 db\, \gamma(b)\, \frac{H(4\,b^2 - E^2)}{\pi\,\sqrt{4\,b^2 - E^2}} \tag{2.63}$$

where in the second relation, there is a change in variables from x to $b(x)$, and $\gamma(b(x)) \equiv b'(x)$ can be defined as the density of values of b. Using the monotonicity assumption, the values

of b vary from some initial b_0 at $x = 0$ to $b = 0$ at $x = 1$. Now, substituting $b = b_0 e^{-\epsilon}$ and $E = E_0 e^{-\epsilon}$, (2.63) becomes

$$\begin{aligned}\rho(E_0\, e^{-\epsilon}) &= \int_0^\infty dz\, b_0\, e^{-z}\, \gamma(b_0\, e^{-z})\, \frac{H(4 - E_0^2\, b_0^{-2}\, e^{2(z-\epsilon)})}{\pi\, b_0\, e^{-z}\, \sqrt{4 - E_0^2\, b_0^{-2}\, e^{2(z-\epsilon)}}} \\ &= \int_0^\infty dz\, b_0\, \gamma(b_0\, e^{-z})\, \frac{H(4 - E_0^2\, b_0^{-2}\, e^{2(z-\epsilon)})}{\pi\, b_0\, \sqrt{4 - E_0^2\, b_0^{-2}\, e^{2(z-\epsilon)}}}\end{aligned} \tag{2.64}$$

This equation is of the form

$$f(\epsilon) = \int_0^\infty dz\, g(z)\, h(\epsilon - z) \tag{2.65}$$

As both f and h are known, we can compute $g(z) = b_0\gamma(b_0 e^{-\epsilon})$ either analytically or numerically. The differential equation $b'(x) = \gamma(b(x))$ can then be solved to obtain $b(x)$.

For the general case where $a(x) \neq 0$, one need to first compute the cumulative density of states (2.61)

$$\begin{aligned}P(E) = \int_{E_{\min}}^{E} dE\, \rho(E) &\approx \int_0^1 dx \int_{E_{\text{left}}(x)}^{E} dE\, \frac{H(4\, b(x)^2 - (E - a(x))^2)}{\pi \sqrt{4\, b(x)^2 - (E - a(x))^2}} \\ &= \int_0^1 dx P_c\left(4 \cdot \frac{E - E_{\text{left}}(x)}{E_{\text{right}}(x) - E_{\text{left}}(x)}\right)\end{aligned} \tag{2.66}$$

where $P_c(z) = \int_{-2}^{z} \frac{1}{\pi\sqrt{4-z'^2}} dz'$ and $P(E)$ are cumulative distributions. The lower limit and upper limit are defined as $E_{left}(x)$ and $E_{right}(x)$ as E is defined only between $E_{right}(x) > E > E_{left}(x)$. The integral in (2.66) can then be numerically solved and in turn be used to solve the values of E_{left}, E_{right}, at m/M from the values at i/M for $i < m$ where x is discretized into M small segments of size $1/M$. The average values of a and b can then be calculated as

$$a \leftarrow \frac{E_{left} + E_{right}}{2}\ ,\ b \leftarrow \frac{E_{left} - E_{right}}{4} \tag{2.67}$$

2.2.3 Statistics of Lanczos coefficients

To study the spectral statistics of a Random Matrix Theory, it is necessary to study the joint probability distribution for the eigenvalues. Similarly, one can contain the joint probability distribution of the Lanczos coefficients. For a Gaussian random matrix, the joint probability distribution is just the product of the probability distribution as the quantities are independent random variables.

$$p_{\text{Gaussian}}(a_0, \cdots, a_{N-1}, b_1, \cdots, b_{N-1}) \propto \left(\prod_{n=0}^{N-1} e^{-\beta N \frac{a_n^2}{4}}\right)\left(\prod_{n=1}^{N-1} b_n^{(N-n)\beta-1} e^{-\beta N \frac{b_n^2}{2}}\right) \tag{2.68}$$

This can be generalized to random matrix ensembles with arbitrary potential $V(H)$ with a modified measure defined as

$$\frac{1}{Z_{\beta,N,V}} e^{-\frac{\beta N}{4}\mathrm{Tr}(V(H))} \tag{2.69}$$

As $\mathrm{Tr}(V(H))$ is invariant under unitary transformations, the joint distribution becomes

$$\begin{aligned} p(a_0,\cdots,a_{N-1},b_1,\cdots,b_{N-1}) &\propto p_{\text{Gaussian}}(a_0,\cdots,a_{N-1},b_1,\cdots,b_{N-1})\,\frac{e^{-\frac{\beta N}{4}\mathrm{Tr}(V(H))}}{e^{-\frac{\beta N}{4}\mathrm{Tr}(H^2)}} \\ &\propto \left(\prod_{n=1}^{N-1} b_n^{(N-n)\beta-1}\right) e^{-\frac{\beta N}{4}\mathrm{Tr}(V(H))} \end{aligned}$$

where $\mathrm{Tr}\big(H^2\big) = \sum_n (a_n^2 + 2b_n^2)$ for tridiagonalized Hamiltonian. The Jacobian of the coordinate transformation from its original form to its tridiagonal form through Lanczos procedure is proportional to

$$J \propto \prod_{n=1}^{N-1} b_n^{(N-n)\beta-1} \tag{2.70}$$

As this applies to one specific sample of a random matrix drawn from the probability distribution, it is the same for any other Gaussian distribution with given β. For generic potential, there is the universal appearance of the Vandermonde determinant. For GOE, the Jacobian that takes the tridiagonal form to the eigenvalue form is

$$J_{T\to\lambda} \propto \frac{\Delta}{\prod_{n=1}^{N-1} b_n^{N-n-1}} \tag{2.71}$$

where Δ is the Vandermonde determinant.

One-point function

At large N, the peak of the probability distribution of the Lanczos coefficients is around the average value. The saddle point approach can thus be used to determine the average and covariance of the Lanczos coefficients. A useful quantity, the logarithm of the probability is defined as effective action as

$$\begin{aligned} S_{\text{eff}} \equiv \ln p(a_0,\ldots,a_{n-1},b_1,\ldots,b_{N-1}) &= \sum_n ((N-n)\beta-1)\ln b_n - \frac{\beta N}{4}\,\mathrm{Tr}(V(H)) \\ &= \sum_n ((N-n)\beta-1)\ln b_n - \frac{\beta N}{4}\,\mathrm{Tr}(V(H)) \end{aligned}$$

The average of the Lanczos coefficients are defined as those which maximize S_{eff}, i.e. the one-point functions. Using $E = a_i b_i x$, few matrix identities and (2.2.2), it is shown in [2] that (2.72) can be represented as

$$S_{\text{eff}} = \sum_n ((N-n)\beta-1)\ln b_n - \frac{\beta N}{4}\sum_n \int dE \frac{V(E)}{\pi\sqrt{4b_n^2-(E-a_n)^2}} \tag{2.72}$$

Introducing Lanczos coefficient as a function $x = n/N$, this effective action in large N-limit gives

$$\frac{S_{\text{eff}}}{\beta N^2} = \int dx(1-x)\ln b(x) - \frac{1}{4}\int dx \int dE \frac{V(E)}{\pi\sqrt{4b(x)^2 - (E-a(x))^2}} \tag{2.73}$$

Assuming polynomial potential form, $V(E) = \sum_n w_n E_n$, the extremum of (2.73) is obtained to find the maximum probability.

$$\begin{aligned} 4(1-x) &= \sum_n w_n \sum_m m a^{n-m} b^{m-1} \binom{n}{m}\binom{m}{m/2} \\ 0 &= \sum_n w_n \sum_m (n-m) a^{n-m-1} b^m \binom{n}{m}\binom{m}{m/2} \end{aligned} \tag{2.74}$$

Thus, given the form of polynomial potential, one can use (2.74) to obtain solutions of Lanczos coefficients with maximum probability.

Two-point function via saddle point approach

The two-point function gives the covariance of the Lanczos coefficients, approximating the probability distribution as a Gaussian around the extremum. The one-point function derived above is used as the extremum point here, expanding the effective action around it to the quadratic term

$$S_{\text{eff}}(a,b) = S_{\text{eff}}(\bar{a},\bar{b}) + \Delta S_{\text{eff}} \tag{2.75}$$

where

$$\Delta S_{\text{eff}} \equiv -\frac{1}{2}(\delta a_i M^{aa}_{ij} \delta a_i + 2\delta a_i\, M^{ab}_{ij} \delta b_i + \delta b_i M^{bb}_{ij} \delta b_i) \tag{2.76}$$

and the kernels are basically blocks from the Hessian matrix

$$\begin{aligned} M^{aa}_{ij} &= \frac{\beta N}{4}\frac{\partial^2}{\partial a_i \partial a_j}\text{Tr}(V(H))r \\ M^{bb}_{ij} &= \frac{\beta N}{4}\frac{\partial^2}{\partial b_i \partial b_j}\text{Tr}(V(H)) - \frac{\partial^2}{\partial b_i \partial b_j}\sum_n((N-n)\beta - 1)\ln b_n \\ M^{ab}_{ij} = M^{ba}_{ji} &= \frac{\beta N}{4}\frac{\partial^2}{\partial a_i \partial b_j}\text{Tr}(V(H)) \end{aligned} \tag{2.77}$$

The covariance or the two-point correlation functions are then calculated from the inverse of these kernels as described in [1].

Chapter 3

The Wigner function

In the standard formulation of quantum mechanics, the probability density $\rho(x)$ in position space x is given by the square of the magnitude of the wave function, $\rho(x) = |\psi(x)|^2$. Similarly, one can find the probability density $\rho(p)$ in momentum space by taking the square of the wave function defined in momentum space given by

$$\phi(p) = \frac{1}{\sqrt{h}} \int e^{-iqp/\hbar} \psi(q) dq \tag{3.1}$$

However, these representations in configuration space (q or p) often present challenges in terms of the evolution of the system, when trying to study the simultaneous behaviour of position and momentum as we do in classical mechanics with Lagrangian and Hamiltonian. Thus, it is desirable to have a wave function defined in phase space (both q and p). In 1932, Eugene Wigner presented the solution to this problem through a mathematical tool known as the Wigner function. The Heisenberg uncertainty principle is conveniently packaged into the Wigner function, asserting constraints on the resulting distribution which satisfies its quantum nature. Another reason to use this quantity is its usefulness in examining the connection between quantum and classical mechanics.

In this section, we will discuss the idea behind Wigner functions and its time evolution. We then look into the discretization of the theory to produce a discrete version of the Wigner function applicable to finite-dimensional Hilbert space. Finally, we will discuss the relation between quantum gates and Wigner functions.

3.1 Wigner formulation of quantum mechanics

Given the standard wavefunction $\psi(q)$, the expectation value of some quantity is obtained by

$$\langle A \rangle = \langle \psi | A | \psi \rangle = \int dx \psi^*(q) \hat{A} \psi(q) \tag{3.2}$$

where $\hat{A}$ is the operator corresponding to A. The operator $\hat{A}$ is a function of the position and the momentum q and p, $\hat{A} \equiv A(q, p)$. The wavefunction $\psi(q)$ describes the probability distribution,

$P(q,p)$, in phase space. Ideally, the desired $P(q,p)$ should be positive everywhere in phase space such that the expectation value is given by

$$\int\int P(q,p)A(q,p)dqdp \tag{3.3}$$

Such a $P(q,p)$ is impossible to find such a quantity in a general sense in the case of quantum mechanics. This is because the Wigner function cannot be a general probability distribution due to the uncertainty principle. Thus, the Wigner function turns out to be a quasi-distribution which can be negative. It should in principle agree with (3.2) to produce expectation value (physical observable).

3.1.1 Weyl transforms and construction of Wigner function

The Weyl transforms are transformations of physical operators to phase space that agrees with the Wigner functions [4]. For an operator $\hat{A}$, the Weyl transform is given by $\tilde{A}$

$$\tilde{A}(q,p) = \int e^{-ipy/\hbar} \langle q + y/2|\hat{A}|q - y/2\rangle \, dy \tag{3.4}$$

where the operator has been expressed in the position basis x. One can similarly express the Weyl transform with the operator in momentum basis p as

$$\tilde{A}(q,p) = \int e^{iqu/\hbar} \langle p + u/2|\hat{A}|p - u/2\rangle \, du \tag{3.5}$$

Thus, the Weyl transform maps an operator from position or momentum space into the phase space.

One interesting property of the Weyl transform is that it relates to the trace of two operators as

$$\mathrm{Tr}\Big[\hat{A}\hat{B}\Big] = \frac{1}{h}\int\int \tilde{A}\tilde{B}dqdp \tag{3.6}$$

Taking one of the operators as density operator, $\hat{\rho} = |\psi\rangle\langle\psi|$ for a pure state $|\psi\rangle$, the identity (3.6) becomes

$$\begin{aligned} \mathrm{Tr}\Big[\hat{\rho}\hat{A}\Big] &= \frac{1}{h}\int\int \tilde{\rho}\tilde{A}dqdp \\ \mathrm{Tr}\Big[\langle\psi|\,\hat{A}\,|\psi\rangle\Big] &= \frac{1}{h}\int\int \tilde{\rho}\tilde{A}dqdp = \langle A\rangle \end{aligned} \tag{3.7}$$

This was the exact idea behind the construction of the Wigner function. Therefore, the Wigner function can be defined as the normalized Weyl transform of the density operator

$$W(q,p) = \frac{\tilde{\rho}}{h} = \frac{1}{h}\int dy \; e^{-ipy/\hbar} \langle q + y/2|\rho(q)|q - y/2\rangle \tag{3.8}$$

From (3.8), one can study the properties of the Wigner function:

- Since the Wigner function depends on both q and p, it is useful to observe how it agrees with the Heisenberg uncertainty principle. For a large value of y, we will have very low uncertainty in p, i.e., W will have a sharp momentum peak but will spread out in the position space. For $y \to 0$, there will be a large value of uncertainty in p, making W spread out in momentum space. It will be more appropriate to rewrite the Wigner function in this case using (3.5)

$$W(q,p) = \frac{1}{h}\int\int e^{iqu/\hbar}\,\langle p+u/2|\hat{\rho(p)}|p-u/2\rangle\,du \tag{3.9}$$

- The Wigner function can produce its corresponding probability density in position or momentum space when integrated in p and q respectively.

$$\begin{aligned}\int W(q,p)dp &= \int dy\;\delta(y)\,\langle q+y/2||\psi\rangle\,\langle\psi||q-y/2\rangle = \psi(q)\psi(q)^*\\ \int W(q,p)dq &= \int du\;\delta(u)\,\langle p+u/2||\phi\rangle\,\langle\phi||p-u/2\rangle = \phi(p)\phi(p)^*\end{aligned} \tag{3.10}$$

- The Weyl transform of $\hat{\mathbf{1}}$ is 1. Using this and the density operator, one can evaluate the integral of Wigner function over both position and momentum space. This is expected to be unity over all phase space.

$$\int\int W(q,p)dqdp = \int\int \tilde{1}W(q,p)dqdp = \mathrm{Tr}\big[\hat{1}\hat{\rho}\big] = 1 \tag{3.11}$$

- For two pure states ψ_a, ψ_b, the corresponding density operator, $\hat{\rho_a}$ and $\hat{\rho_b}$, one can find the trace to be

$$\begin{aligned}h^{-1}\,\mathrm{Tr}[\hat{\rho_a}\hat{\rho_b}] &= \int\int W_a(q,p)W_b(q,p)dqdp\\ h^{-1}|\langle\psi_a|\psi_b\rangle|^2 &= \int\int W_a(q,p)W_b(q,p)dqdp\end{aligned} \tag{3.12}$$

  The quantity on left-hand side will be zero for orthogonal states. Thus, the Wigner function needs to be negative for some regions of phase space.

- One can define two normalized wavefunction of y, $\psi_1(y) = e^{-ipy/\hbar}\psi(q+y/2)/\sqrt{2}$ and $\psi_2(y) = \psi(q-y/2)/\sqrt{2}$. The Wigner function can then be represented as

$$W(q,p) = \frac{2}{2\pi\hbar}\int \psi_1(y)\psi_2(y)dy \tag{3.13}$$

  which implies that $|W(q,p)| \leq 1/\pi\hbar$. thus, the Wigner function cannot take arbitrarily large values in phase space as opposed to a classical distribution.

3.1.2 Time dependence of Wigner function

Next, it would be useful to study the time dependence of Wigner function. By taking the derivative of (3.8) with respect to time

$$\frac{\partial W}{\partial t} = \frac{1}{h}\int dy\, e^{-ipy/\hbar}\left[\frac{\partial \psi^*(q-y/2)}{\partial t}\psi(q+y/2) + \frac{\partial \psi(q+y/2)}{\partial t}\psi^*(q-y/2)\right] \tag{3.14}$$

Using Schrödinger equation, (3.14) can be represented as

$$\frac{\partial W}{\partial t} = \frac{\partial W_T}{\partial t} + \frac{\partial W_U}{\partial t} \tag{3.15}$$

where

$$\begin{aligned}\frac{\partial W_T}{\partial t} &= \frac{1}{4\pi i m}\int dy\, e^{-ipy/\hbar}\left[\frac{\partial^2 \psi^*(q-y/2)}{\partial q^2}\psi(q+y/2) - \frac{\partial^2 \psi(q+y/2)}{\partial q^2}\psi^*(q-y/2)\right] \\ \frac{\partial W_U}{\partial t} &= \frac{2\pi}{ih^2}\int dy\, e^{-ipy/\hbar}[U(q+y/2) - U(q-y/2)]\psi^*(q-y/2)\psi(q+y/2)\end{aligned} \tag{3.16}$$

Each of these terms can be simplified as shown in [3]

$$\begin{aligned}\frac{\partial W_T}{\partial t} &= -\frac{p}{m}\cdot\frac{\partial W(q,p)}{\partial q} \\ \frac{\partial W_U}{\partial t} &= \sum_{s=0}^{\infty}\left(-\hbar^2\right)^s \cdot \frac{1}{(2s+1)!}\left(\frac{1}{2}\right)^{2s}\cdot\frac{\partial^{2s+1}U(q)}{\partial q^{2s+1}} \times \left(\frac{\partial}{\partial p}\right)^{2s+1} W(q,p)\end{aligned} \tag{3.17}$$

Within first order approximation, all derivatives of $U(q)$ higher than second order are negligible [4], transforming (3.17) into

$$\frac{\partial W_U}{\partial t} = \frac{\partial U(q)}{\partial q}\frac{\partial W(q,p)}{\partial p} \tag{3.18}$$

With this approximation, the governing equation for the time evolution of Wigner function becomes

$$\frac{\partial W(q,p)}{\partial t} = -\frac{p}{m}\frac{\partial W(q,p)}{\partial q} + \frac{\partial U(q)}{\partial q}\frac{\partial W(q,p)}{\partial p} \tag{3.19}$$

3.2 Wigner function in terms of phase-point operators

In the next section, we are required to make the transition from the continuous Wigner function to the discrete case. It is convenient to express the continuous Wigner function in terms of "phase-point operators"[7]. Let $\hat{A}(q,p)$ be phase-point operator associated with the phase coordinate (q,p), such that

$$\hat{\rho} = \int W(q,p)\hat{A}(q,p)dqdp \tag{3.20}$$

To satisfy (3.8), the *phase-point operator* $\hat{A}(q,p)$ must take the form

$$\langle q' | \hat{A}(q,p) | q" \rangle = \delta \left(q - \frac{q' + q"}{2} \right) e^{-\frac{ip}{\hbar}(q'-q")}. \tag{3.21}$$

These operators can also be expressed in terms of their components in momentum basis.

$$\langle p' | \hat{A}(q,p) | p" \rangle = \delta \left(p - \frac{p' + p"}{2} \right) e^{-\frac{iq}{\hbar}(p'-p")}. \tag{3.22}$$

These phase-point operators have similar properties corresponding to that of the Wigner function that were stated in the previous section.

1. For each phase-point (q,p), the trace is $\mathrm{Tr}\Big(\hat{A}(q,p)\Big) = 1$, which ensures the normalization of the Wigner function.

2. The phase-point operators corresponding to two different phase point (q_1,p_1) and (q_2,p_2) have a joint trace of

$$\mathrm{Tr}\Big[\hat{A}(q_1,p_1)\hat{A}(q_2,p_2)\Big] = 2\pi\hbar\ \delta(q_1-q_2)\delta(p_1-p_2) \tag{3.23}$$

which shows that the $\hat{A}$'s are a set of orthonormal operators, under the inner product given by the trace of the operator product [7]. They also form a complete set, spanning all phase space, i.e., any Hermitian operator can be written as a real linear combination of them.

3. **Projection property:** For a particle in one dimension, consider the integral of W over the infinite strip bounded by two parallel lines in phase space, say $aq + bp = c_1$ and $aq + bp = c_2$. The integral gives the probability of finding the observable $a\hat{q} + b\hat{p}$ between c_1 and c_2 [7]. The projection operator $\hat{P}$ is given by

$$\hat{P} = \frac{1}{2\pi\hbar} \int\int_{strip} \hat{A}(q,p)\ dq\ dp \tag{3.24}$$

which projects onto the subspace spanned by the eigenstates of the operator $a\hat{q} + b\hat{p}$ with eigenvalues lying between c_1 and c_2.

The Wigner function can be explicitly expressed in terms of phase-point operators and the density operator as follows:

$$W(q,p) = \frac{1}{2\pi\hbar}\,\mathrm{Tr}\Big[\hat{\rho}\hat{A}(q,p)\Big] \tag{3.25}$$

Thus, the Wigner function at any point is proportional to the expectation value of the phase-point operator $\hat{A}(q,p)$ associated with that point.

The phase-point operators are also related to the *Heisenberg-Weyl* (HW) displacement operators. The Heisenberg-Weyl group consists of unitary operators generated by translations in position and momentum space, corresponding to the classical symmetries of phase space.

$$\begin{aligned} w(q,p) = e^{\frac{i}{\hbar}(p\mathbf{q}-q\mathbf{p})} = e^{-\frac{i}{2\hbar}pq} Z(p)X(q) \\ Z(p) = e^{\frac{i}{\hbar}p\mathbf{q}}, X(q) = e^{-\frac{i}{\hbar}q\mathbf{p}} \end{aligned} \tag{3.26}$$

where $\mathbf{q}$ and $\mathbf{p}$ are phase operators, conjugate position and momentum, which satisfy $[\mathbf{q}, \mathbf{p}] = i\hbar$. The phase-point operators are then the symplectic Fourier transform of the HW operators:

$$A(q,p) = \int \frac{dp'dq'}{2\pi\hbar} e^{\frac{i}{\hbar}(p'q-q'p)} w(q',p') \tag{3.27}$$

Using, phase-point operators, we can redefine the time evolution of the Wigner function given by the Moyal equation, which reduces to the Liouville equation in the limit $\hbar \to 0$

$$\begin{aligned} \frac{dW}{dt} &= \frac{2}{\hbar} \sin\left(\frac{\hbar}{2}(\partial_{x'}\partial_p - \partial_{p'}\partial_x)\right) h(x',p')W(x,p)\Big|_{x'=x,p'=p} \\ &= \{h, W\}_{PB} + O(\hbar) \end{aligned}$$

where $h(x,p)$ can be defined as the Weyl transform of the Hamiltonian H.

In quantum mechanics, the uncertainty principle dictates that certain pairs of observables, such as position and momentum, cannot be simultaneously determined with arbitrary precision. As a result, the Wigner function can take negative values in regions of phase space where quantum interference effects are prominent. Thus, the non-positivity of the Wigner function arises from the inherently non-classical nature of quantum mechanics. Hudson's theorem shows that the only states for which the Wigner function is everywhere positive are the Gaussian states [3],

$$\psi(q) \sim e^{-\frac{1}{2}aq^2 - bq}. \tag{3.28}$$

where $a, b \in \mathbb{C}$. These states are characterized by their narrow width in both position and momentum space, leading to a spread-out Wigner function that is always positive. The positivity of the Wigner function for Gaussian states arises from their phase-space distribution being smooth and well-behaved, without the interference effects present in more general quantum states. These form a closed restricted class of states in the Hilbert space. The connection between this restricted class of the Wigner function and classicality can be further understood in the context of the Heisenberg-Weyl group and the Clifford group. These HW operators form the basis for the Clifford group, which includes additional symmetries such as rotations and

reflections. Gaussian states are invariant under operations of the Clifford group, leading to a positive-definite Wigner function that reflects the classical-like behaviour of these states.

3.3 Discrete Wigner function

The previous sections focused on infinite-dimensional Hilbert spaces. Our main focus is to develop the Krylov-Wigner function, which is defined in quantum systems with finite Hilbert spaces having exactly D orthogonal states. To complete the assignment, one needs a discrete version of phase space and phase point operators [7]. A discrete phase space $\mathcal{P}$ is defined as a lattice of size $D \times D$, where D is the dimension of the Hilbert space. It is simplest and most effective to consider the case where D is a prime number and treat composite D's by some power of a prime or embedding it in a larger Hilbert space with prime dimension.

In this finite phase space, lines connecting different phase points (q_i, p_j) and parallel lines become important. All the addition and multiplication of elements in this finite field are $\mod D$. A complete set of N parallel lines is called a "*foliation*" of phase space. For a D dimensional lattice, we have $D+1$ different sets of foliations. The phase space $\mathcal{P}$ is then defined as $\mathbb{Z}_D \times \mathbb{Z}_D$, with a symplectic inner product between two points $\vec{\alpha} = (q, p)$ and $\vec{\beta} = (q', p')$ given by:

$$\left[\vec{\alpha}, \vec{\beta}\right] = pq' - qp' \tag{3.29}$$

The next step is to study the discrete version of Weyl operators and thus the phase-point operators. Let $\{\, |k\rangle \,\}_{k=0}^{D-1}$ be a chosen orthonormal basis for the Hilbert space. In terms of this basis, a discrete version of the Heisenberg-Weyl (HW) operators:

$$w(q,p) = e^{-\frac{2\pi i}{D}\frac{D+1}{2}qp} Z(p)X(q) \tag{3.30}$$

where $(q,p) \in \mathcal{P}$ and the boost and shift operators are defined as

$$X(q)\,|q'\rangle = \left|q' + q \mod D\right\rangle \ , \ Z(p)\,|q\rangle = e^{\frac{2\pi i p q}{D}} \tag{3.31}$$

The HW operators have the property of being closed under multiplication as in the continuous case. It can be observed that

$$w(p,q)w(q',p') = e^{\frac{2\pi i}{D}\frac{(pq'-qp')}{2}} w(q+q', p+p') \tag{3.32}$$

It should also be noted that the discussion on the Clifford group applies here also, i.e., up to a phase, the Clifford operators take the HW operators to themselves. This will be discussed in the

later section.

As in the continuous case, the phase-point operators are just the symplectic Fourier transform of the HW operators, which applies in the discrete case also:

$$A(q,p) = \sum_{k,\ell=0}^{D-1} \widehat{\delta}_{2q,k+l} e^{\frac{2\pi i}{D}(k-\ell)p} \tag{3.33}$$

where the Kronecker delta operator $\hat{\delta}$ follows the mod rule, i.e., $(k+l) = 2q \mod D$ and zero otherwise. These phase point operators $A_{\vec{\alpha}}$ associated with some phase point $\vec{\alpha} = (q,p)$ can be thought of as an $D \times D$ matrix operator. They have the following properties:

1. For each point $\vec{\alpha}$, $\mathrm{Tr}(A_{\vec{\alpha}}) = 1$,
2. For any two points $\vec{\alpha}$ and $\vec{\beta}$, $\mathrm{Tr}\Big(A_{\vec{\alpha}\vec{\beta}}\Big) = D\delta_{\vec{\alpha}\vec{\beta}}$,
3. The D projection operators, in this case, are a set of mutually orthogonal operators whose sum is the identity,

$$\frac{1}{D}\sum_{\vec{\alpha}} A_{\vec{\alpha}} = 1. \tag{3.34}$$

Now that we have the phase space as well as the phase-point operators well-defined for discrete systems, the discrete Wigner function can be defined in terms of these. The discrete Wigner function of a state $\rho \in L(\mathcal{C}^D)$ is a quasi-probability distribution over $(\mathcal{Z}_D \times \mathcal{Z}_D)$ as

$$W_\rho(\vec{\alpha}) = \frac{1}{D}\,\mathrm{Tr}(\rho A_{\vec{\alpha}}) \tag{3.35}$$

This is derived from inverting the definition of the density matrix, where the Wigner function is defined as a set of coefficients in its expansion $\rho = \sum_{\vec{\alpha}} W_{\vec{\alpha}} A_{\vec{\alpha}}$. It has the following properties

1. The discrete Wigner function is real and normalized

$$\sum_{\vec{\alpha}} W_\rho(\vec{\alpha}) = \mathrm{Tr}\left(\rho \sum_{\vec{\alpha}} \frac{1}{D} A_{\vec{\alpha}}\right) \implies \mathrm{Tr}(\rho) = 1 \tag{3.36}$$

2. Summing the Wigner function over one of the directions x or p, say p, reduces it to the discrete probability density along the other direction

$$\sum_{p=0}^{D-1} W_\rho(x,p) = \langle x|\rho|x\rangle \tag{3.37}$$

It follows synonymously from the projection property in the continuous case, that summation along any foliation gives us the probability of the outcome of a specific measurement associated with the given foliation. In this case, the foliation is parallel to x or p, giving the probability density along p or x respectively.

The time evolution of the system is generated by a $D \times D$ Hermitian operator $\hat{H}$ along the lines of

$$\frac{\mathrm{d}\hat{\rho}}{\mathrm{d}t} = i[\hat{\rho}, \hat{H}] \tag{3.38}$$

Substituting the expression for ρ in terms of W, one can find the time evolution of the Wigner function. With the Hamiltonian defined in terms of phase point operators, $H = \sum_{\vec{\alpha}} H(\vec{\alpha}) A_{\vec{\alpha}}$, (3.38) becomes

$$\begin{aligned} \frac{\mathrm{d}}{\mathrm{d}t} \sum_{\vec{\alpha}} W_{\vec{\alpha}} A_{\vec{\alpha}} &= i[\sum_{\vec{\beta}} W(\vec{\beta}) A_{\vec{\beta}}, \sum_{\vec{\gamma}} H(\vec{\gamma}) A_{\vec{\gamma}}] \\ \sum_{\vec{\alpha}} \frac{\mathrm{d}W_{\vec{\alpha}}}{\mathrm{d}t} A_{\vec{\alpha}} &= i \sum_{\vec{\beta}\vec{\gamma}} [A_{\vec{\beta}}, A_{\vec{\gamma}}] H(\vec{\beta}) W_\rho(ga\vec{m}ma) \\ \frac{\mathrm{d}W_\rho(\vec{\alpha})}{\mathrm{d}t} &= -\frac{i}{D} \sum_{\vec{\beta},\vec{\gamma}} \mathrm{Tr}\left(A_{\vec{\alpha}} \left[A_{\vec{\beta}}, A_{\vec{\gamma}}\right]\right) H(\vec{\beta}) W_\rho(\vec{\gamma}) \end{aligned} \tag{3.39}$$

where in the third line, we invert the equation as before in (3.35), where the quantity $1/D \,\mathrm{Tr}\left(A_{\vec{\alpha}} \left[A_{\vec{\beta}}, A_{\vec{\gamma}}\right]\right)$ has some interesting properties. This quantity is defined as a complex function $\Gamma_{\vec{\alpha}\vec{\beta}\vec{\gamma}}$ which is *cyclic* and *real* with respect to the indices and in the case of prime $D > 2$ has the form

$$\Gamma_{\vec{\alpha}\vec{\beta}\vec{\gamma}} = \frac{1}{D} \exp\left(\frac{4\pi i}{D} \mathcal{A}_{\vec{\alpha}\vec{\beta}\vec{\gamma}}\right) \tag{3.40}$$

where

$$\mathcal{A}_{\vec{\alpha}\vec{\beta}\vec{\gamma}} = \alpha_2(\gamma_1 - \beta_1) + \beta_2(\alpha_1 - \gamma_1) + \gamma_2(\beta_1 - \alpha_1), \tag{3.41}$$

This reduces the time evolution of the discrete Wigner function to a discrete version of the Moyal equation:

$$\frac{dW_\rho(\vec{\alpha})}{dt} = \frac{2}{D} \sum_{\vec{\beta},\vec{\gamma}} \sin\left(\frac{4\pi}{D} \mathcal{A}_{\vec{\alpha}\vec{\beta}\vec{\gamma}}\right) H(\vec{\beta}) W_\rho(\vec{\gamma}), \tag{3.42}$$

3.4 Wigner Negativity

3.4.1 Wigner positivity and quantum circuit

The discrete Wigner function being a quasi-probability distribution can take negative values as well. As discussed in the continuous case, the states with discrete non-negative Wigner functions similarly are Gaussian states as stated in Hudson's theorem.

$$\langle q|\psi\rangle \sim e^{\frac{2\pi i}{D}(aq^2 + bq)} \tag{3.43}$$

where $a, b \in \mathbb{Z}_D$. Naturally, the corresponding Wigner functions are highly constrained. To define the functions precisely, consider a subspace $\mathcal{L}$ of phase space. This is an isotropic subspace if for any $\vec{\alpha}, \vec{\beta} \in \mathcal{L}$, we have

$$\left[\vec{\alpha}, \vec{\beta}\right] = 0 \tag{3.44}$$

The product rule of HW operators shows that the HW group elements corresponding to an isotropic subspace form a subgroup. The Clifford operators $U \in C_D$ are the unitary operators that, up to a phase, map Heisenberg-Weyl operators to themselves. The set of all such operators forms a group, known as the Clifford group for dimension D. The positivity in the discrete case is constrained and implies that the Wigner function has to be of the form [3]

$$W_\psi(q,p) = \begin{cases} \frac{1}{D} & \cdots \text{ if } (q,p) \in \mathcal{L} \\ 0 & \cdots \text{ if } (q,p) \notin \mathcal{L}, \end{cases} \tag{3.45}$$

where $\mathcal{L}$ is some maximally isotropic subspace.

Starting with a Gaussian state, the positivity of the Wigner function isn't generally conserved under time evolution. Only specific types of operators, i.e., the Clifford operators, conserve the positivity in time evolution.

Such states with non-negative Wigner function that are invariant under Clifford operations are called "stabilizer states". Pure stabilizer states for the D dimension are defined as the set of states

$$S_i = \{\, U\,|\psi_0\rangle \;:\; U \in C_d \,\} \tag{3.46}$$

and a full set of stabilizer states be $\sigma = \sum_i p_i S_i \;: \sigma \in L(\mathcal{H}_\mathcal{D})$, for some probability distribution p_i. These stabilizer states and operations are a subset of a larger class of a full set of allowed quantum operations on a finite-dimensional system. A system with an initial state that can be represented in terms of stabilizer states, i.e., $|\psi\rangle = \sum_i c_i S_i$, is thus guaranteed to have a non-negative Wigner function. Any quantum evolution involving such an initial state and only Clifford gates will keep the state within the restricted class. Thus, one can keep track of the evolution of the finite set of Lanczos parameters, $(a(t), b(t))$ instead of the entire wavefunction. Therefore, such systems can be efficiently simulated on a classical computer.

The "Clifford group" is defined more precisely as a subset of unitary operators which map HW operators to HW operators:

$$U w(\vec{\alpha}) U^\dagger = w(S(\vec{\alpha})) \tag{3.47}$$

for some $S : \mathcal{P} \to \mathcal{P}$. Clifford unitaries act as permutations of phase space. But only a small subset of the possible permutations of phase space correspond to Clifford operations, i.e., the symplectic ones. A *symplectic* transformation $S : \mathcal{P} \to \mathcal{P}$ on phase space is a linear map (with coefficients in $\mathbb{Z}_D$) which preserves the symplectic inner product:

$$\left[S(\vec{\alpha}), S(\vec{\beta})\right] = \left[\vec{\alpha}, \vec{\beta}\right]. \tag{3.48}$$

Corresponding to every symplectic map, there exists a unitary operator $\mu(S)$ such that

$$\mu(S)\, w(\vec{\alpha})\, \mu(S)^\dagger = w(S(\vec{\alpha})). \tag{3.49}$$

Up to a phase, every Clifford unitary is of the form $U = w(\vec{\alpha})\, \mu(S)$. Thus, the Clifford group is essentially a representation of the group of symplectic affine transformations on phase space. The Wigner function transforms covariantly under the Clifford group, namely

$$W_{U\psi}(\vec{\beta}) = W_\psi(S(\vec{\beta}) + \vec{\alpha}). \tag{3.50}$$

The concept of Wigner functions extends to quantum operations or channels, where they provide valuable insights. The Clifford operators can be represented analogously by quantum gates and more appropriately by quantum channels. It is shown that a quantum circuit consisting of an initial quantum state, unitary evolution, and measurements, each having non-negative Wigner functions, can be classically simulated[6]. Consider a quantum channel $\mathcal{E}$, which maps states from an input space $\mathcal{H}$in to an output space $\mathcal{H}$out. The corresponding Choi-Jamiolkowski (CJ) state, denoted as $\sigma_\mathcal{E}$, is defined as follows:

$$\sigma_\mathcal{E} = (\mathbf{1} \otimes \mathcal{E})(|\Omega\rangle\langle\Omega|), \tag{3.51}$$

where $|\Omega\rangle = \sum_{k=1}^{D} |k\rangle \otimes |k\rangle$ represents the maximally entangled state on two copies of the Hilbert space.

This CJ state encodes a complete portrayal of the quantum channel $\mathcal{E}$, encapsulating all details about its behaviour on arbitrary input states. Subsequently, the discrete Wigner function of the channel $\mathcal{E}$ is defined as:

$$W_\mathcal{E}(\vec{\beta}|\vec{\alpha}) = \frac{1}{D}\mathrm{Tr}\left(A_{\vec{\alpha}}^T \otimes A_{\vec{\beta}}, \sigma_\mathcal{E}\right) = \frac{1}{D}\mathrm{Tr}\left(A_{\vec{\beta}}, \mathcal{E}(A_{\vec{\alpha}})\right), \tag{3.52}$$

where $A_{\vec{\alpha}}$ and $A_{\vec{\beta}}$ are operators associated with phase space points $\vec{\alpha}$ and $\vec{\beta}$, respectively.

Furthermore, given an input state ρ with Wigner function $W_\rho(\vec{\alpha})$, the Wigner function of the output state $\mathcal{E}(\rho)$ can be expressed as follows:

$$W_{\mathcal{E}(\rho)}(\vec{\beta}) = \sum_{\vec{\alpha}} W_{\mathcal{E}}(\vec{\beta}|\vec{\alpha}) W_\rho(\vec{\alpha}). \tag{3.53}$$

A quantum measurement with positive operator valued measure (POVM) M_k is represented by assigning quasi-probability functions over the phase space to each measurement outcome

$$W_k(\vec{\alpha}) = \mathrm{Tr}\left(M_k, A_{\vec{\alpha}}\right). \tag{3.54}$$

where $W_k(\vec{\alpha}) \geq 0$. This can be interpreted classically as a projection function associated with classical outcome, i.e., the probability of getting a particular outcome given that the 'physical state' is at phase space point $\vec{\alpha}$.

Thus, it's evident that Wigner functions can be attributed to various elements within a quantum circuit, providing a versatile tool for analysis. As already mentioned, according to *Gottesman-Knill theorem*, any quantum circuit that is initialized to a stabilizer state and involves only Clifford operators evolves within a very restricted subset of the Hilbert space and such quantum circuits can be simulated efficiently on a classical computer. Now, any circuit initializing with a stabilizer state and measurements defined by POVM M_k with a positive Wigner function can be represented with circuit elements on a classical computer. Given initial state ψ_0, the Wigner function for each operation constitutes a stochastic matrix, and the Wigner function for each POVM M_k constitutes a probability over k for each point in phase space. The outcome of the quantum circuit is given as

$$P_k = \mathrm{Tr}\left(M_k \, \mathcal{E}_m \cdots \mathcal{E}_1(|\psi_0\rangle\langle\psi_0|)\right), \tag{3.55}$$

which translates to classical stochastic evolution in terms of the Wigner function representations[3]:

$$P_k = \sum_{\vec{\alpha}} \sum_{\vec{\beta_1} \cdots, \vec{\beta}_m} \sum_{\vec{\gamma}} W_{M_k}(\vec{\alpha}) \, W_{\mathcal{E}_m}(\vec{\beta_m}|\vec{\beta}_{m-1}) \cdots W_{\mathcal{E}_1}(\vec{\beta_1}|\vec{\gamma}) \, W_{\psi_0}(\vec{\gamma}). \tag{3.56}$$

3.4.2 The idea of Wigner Negativity

As discussed in the previous section, any non-negative Wigner function can be regarded as an initial stabilizer state with Clifford operators acting on it. Since the positivity corresponds to the classical nature of the system, the negativity of the Wigner function is a measure of "inherent

quantumness". So, to construct a quantum circuit that represents not only the non-negative Wigner function but also the negativity, one needs to consider the transformation of non-stabilizer states. *A state is **magic** if it is not a stabilizer state* [5]. It is helpful to introduce resource theory to deal with non-stabilizer states. Resource theory provides a rigorous framework for studying and understanding the manipulation, transformation, and quantification of various physical quantities and states. Here, within the resource theory of stabilizer states, stabilizer states can be viewed as *free states* that can be transformed using *stabilizer operations* without consuming any additional resources. Stabilizer operations include operations that preserve the stabilizer subgroup of the Pauli group, such as Clifford gates and measurements in the Pauli basis. Since stabilizer states are stabilized by the maximally isotropic subgroup of the Heisenberg-Weyl group, they possess non-negative Wigner functions and exhibit certain desirable properties, such as being efficiently simulatable on classical computers. For a function to be a valid measure of magic, i.e. a monotone, it must be non-increasing under stabilizer operations. This can be formalized as follows[5]:

> *For D dimensional Hilbert space, let $\mathcal{M}_D : S(\mathcal{H}_D) \to \mathbb{R}$ be mapping from the set of density operators on $\mathcal{H}_D$ to real numbers. A specific quantity $\mathcal{M}$ is defined as $\mathcal{M}(\rho) \equiv \mathcal{M}_D(\rho)\ \forall\, \rho \in S(\mathcal{H}_D)$ so that $\mathcal{M}(\cdot)$ is defined for all finite-dimensional Hilbert spaces.*

If Λ is a stabilizer protocol involving some measurement, and

$$\Lambda(\rho) = \sum_i p_i \sigma_i \tag{3.57}$$

where σ_i are sets of stabilizer states with probability p_i. The quantity $\mathcal{M}$ is called a *magic monotone* if

$$\mathcal{M}(\rho) \geq \sum_i p_i \mathcal{M}(\sigma_i) \tag{3.58}$$

and $\mathcal{M}(S) = 0$ for all stabilizer states. So, even if $\mathcal{M}_\rho < \mathcal{M}(\sigma_i)$, one requires the monotone operations not to increase magic on average.

It is shown in [5] that the sum negativity of a state ρ, i.e., the absolute value of the sum of the negative entries of the discrete Wigner function, is a magic monotone. Since sum negativity is clearly 0 for all stabilizer states, they can be included in the sum, it can be redefined as

$$\mathcal{N}(\psi) = \sum_{x,p} |W_\psi(x,p)| \tag{3.59}$$

which is non-increasing under stabilizer operations. It is more suitable to define the logarithm of the sum negativity of Wigner function, known as *mana*:

$$\mathcal{M}(\psi) = \log \mathcal{N}(\psi) \tag{3.60}$$

The logarithmic negativity has several nice properties.

1. By definition, the log-negativity is positive definite and is zero if and only if the Wigner function is nowhere negative, i.e., for Gaussian-like states.

2. The log-negativity is also bounded above by $\frac{1}{2}\log D$. From (3.3), it is easy to observe that

$$\sum_{\vec{\alpha}} W_{\vec{\alpha}}^2 = \frac{1}{D}\operatorname{Tr}\left(\rho^2\right) \tag{3.61}$$

   It is a fact that for stabilizer states $\operatorname{Tr}\left(\rho^2\right) = \operatorname{Tr}(\rho) = 1$, where for general states including non-stabilizer states $\operatorname{Tr}\left(\rho^2\right) < 1$. Together with Jensen's inequality, this implies

$$\sum_{\vec{\alpha}} |W_{\vec{\alpha}}| \leq D\sqrt{\sum_{\vec{\alpha}} W_{\vec{\alpha}}^2} = \sqrt{D}\sqrt{\operatorname{Tr}\rho^2} \leq \sqrt{D} \tag{3.62}$$

3. It facilitates *magic distillation*. Any stabilizer protocol Λ which consumes resource states ρ to produce m copies of a target state σ with some finite probability, requires, on average, at least $m\frac{\mathcal{M}(\sigma)}{\mathcal{M}(\rho)}$ copies of ρ [5]. This follows from the fact that mana is additive under tensor factorization, $\mathcal{M}(\rho \otimes \sigma) = \mathcal{M}(\rho) + \mathcal{M}(\sigma)$, and that the log-negativity decreases on average under stabilizer operations.

It should also be noted that sum negativity is the best and unique way to quantify the magic of a state by the negativity of its Wigner representation. Thus, the negativity of the Wigner function constitutes an operationally meaningful notion of the inherent "quantumness" of a state. In the rest of this work, we will mainly focus on the negativity as opposed to the log-negativity:

$$\mathcal{N}(\psi) = \sum_{x,p} |W_\psi(x,p)|, \tag{3.63}$$

and regard it as a measure of the non-classicality or "quantumness" of a state.

Chapter 4

The Krylov-Wigner (KW) function

The exploration of quantum systems in the context of quantum gravity has led to fascinating connections between seemingly disparate fields. One such intriguing connection arises in the study of the double-scaled SYK (DSSYK) model, a model of Majorana fermions with all-to-all p-body interactions. The couplings in the Hamiltonian are chosen randomly from a Gaussian ensemble, and one takes a double-scaling limit where $p \to \infty$, $N \to \infty$ with $\lambda = \frac{2p^2}{N}$ fixed. In the DSSYK model, a remarkable phenomenon happens: the emergence of JT gravity in a particular triple scaling limit. Central to understanding the intricacies of the DSSYK model is the notion of a basis in which calculations can be effectively organized. In recent research, a basis known as the "chord-number" basis has been identified as the natural framework for studying the DSSYK model. This basis, which finds its roots in the gravitational length basis of JT gravity, offers a structured approach to exploring the dynamics of the system.

Remarkably, from the perspective of the boundary quantum system, the chord-number basis reveals itself to be none other than the Krylov basis. This revelation raises intriguing questions about the underlying connection between the gravitational variables and the Krylov basis. Thus, it is natural to study what makes the Krylov basis special. Given that the Wigner function's definition extends to any orthonormal basis, it follows that it could potentially be defined within the framework of the Krylov basis as well.

4.1 Setting the groundwork

From the results of [2], it is shown that the Krylov basis minimizes the complexity of a given quantum system for all bases. Thus, it is natural that the time-dependent wavefunction tends to concentrate maximally on this basis, i.e., the state exhibits a behaviour that can be described as "classical", although described in phase space. To investigate this notion further and understand how the Krylov basis maximizes the classicality of the evolving state, it is prudent to delve into the evolution dynamics in phase space, as discussed in Section (2.1). In line with this

approach, we define a discrete phase space $\mathcal{P} = \mathbb{Z}_D \times \mathbb{Z}_D$ relative to the Krylov basis, where each point (q, p) corresponds to a basis element. Here, q and p represent discrete analogs of position and momentum, respectively. We introduce a Wigner function, denoted $W\psi(q, p)$, which characterizes the state ψ in this phase space. Formally, this function is given by:

$$W_\psi(q,p) = \frac{1}{D} \sum_{k,\ell=0}^{D-1} \widehat{\delta}_{2q,k+\ell} e^{\frac{2\pi i}{D}(k-\ell)p} \langle k|\psi\rangle\langle\psi|\ell\rangle. \tag{4.1}$$

Our primary interest lies in understanding the Wigner function of the time-evolved initial state $|\psi(t)\rangle = e^{-iHt}|\psi_0\rangle$. This quantity is termed the *Krylov-Wigner function* [3], offering a quantitative means to examine the evolution of the density operator $|\psi\rangle\langle\psi|$ across the discrete Krylov phase space. To accomplish this, we need to identify discrete phase-point operators corresponding to the Krylov basis and then expand the evolved density matrix $|\psi(t)\rangle\langle\psi(t)|$ in terms of these operators.

Obtaining the discrete Wigner functions of the evolved wave function can be approached in two distinct ways. Firstly, we can analyze the operator evolution within the discrete Krylov basis, akin to the operator version of the Krylov basis as discussed in the context of Krylov-Operator Complexity. This involves constructing a set of operators $\{\rho, [H,\rho], [H,[H,\rho]], \cdots\}$, where $\rho = |\psi\rangle\langle\psi|$. Alternatively, the second approach focuses on directly expanding the evolved density matrix itself, employing the Lanczos procedure derived from the study of the evolved wave function rather than the operators. The Krylov-Wigner function emerges as the corresponding wavefunction in the basis formed by phase-point operators. These methodologies offer complementary insights into the evolution dynamics of quantum systems within the Krylov framework, facilitating a comprehensive understanding of the Krylov-Wigner function and its implications. Thus, for the Wigner function evolving with time, we can do a Taylor expansion in t:

$$W_{\psi(t)} = W_{\psi(0)} + t\,\frac{\partial W_{\psi(t)}}{\partial t}\bigg|_{\psi(0)} + t^2\,\frac{\partial^2 W_{\psi(t)}}{\partial t^2}\bigg|_{\psi(0)} + \cdots \tag{4.2}$$

The KW function at time $t = 0$ is given by

$$W_{\psi_0}(q,p) = \frac{1}{D}\delta_{q,0}. \tag{4.3}$$

Here, k and l takes the value 0 for $t = 0$ reducing the delta function to $\delta_{q,0}$. For the next term,

we have

$$\begin{aligned}\left.\frac{\partial W_{\psi(t)}}{\partial t}\right|_{\psi(0)} &= \frac{1}{D}\sum_{k,l}^{D-1}\widehat{\delta}_{2q,k+l}e^{2\pi i(k-l)p/D}\frac{\partial}{\partial t}\langle k|\psi\rangle\langle\psi|l\rangle \\ &= -\frac{i}{\hbar D}\sum_{k,l}^{D-1}\widehat{\delta}_{2q,k+l}e^{2\pi i(k-l)p/D}H\langle k|\psi\rangle\langle\psi|l\rangle \\ &= -\frac{i}{\hbar D}\sum_{k,l}^{D-1}\widehat{\delta}_{2q,k+l}e^{2\pi i(k-l)p/D}\left[\langle k|H|0\rangle\langle 0|l\rangle - \langle k|0\rangle\langle 0|H|l\rangle\right]\end{aligned} \tag{4.4}$$

For the second term, we have $k+l=1$ with $k=0,\ l=1$ and $k=1,\ l=0$. The phase turns out to be $\exp\left(\pm\frac{2\pi ip}{D}\right)$. Thus, the second term turns out to be

$$-\frac{2t}{D}\widehat{\delta}_{2q,1}\sin\left(\frac{2\pi p}{D}\right) \tag{4.5}$$

Thus, the general representation for the Krylov-Wigner function can be given as a Taylor expansion in t:

$$\begin{aligned}W_{\psi(t)}(q,p) &\simeq \frac{1}{D}\delta_{q,0} - \frac{it}{D}\sum_{k,\ell}\widehat{\delta}_{2q,k+\ell}e^{\frac{2\pi i}{D}(k-\ell)p}\left(\langle k|H|0\rangle\langle 0|\ell\rangle - \langle k|0\rangle\langle 0|H|\ell\rangle\right) + \cdots \\ &= \frac{1}{D}\delta_{q,0} - \frac{2t}{D}\widehat{\delta}_{2q,1}\sin\left(\frac{2\pi p}{D}\right) + \cdots .\end{aligned} \tag{4.6}$$

It's interesting to note that the second term in the expression (4.6) becomes non-zero only under unique circumstances. In the discrete phase space $\mathcal{P} = \mathbb{Z}_D \times \mathbb{Z}_D$, the position coordinates span from $q=0$ to $q=D-1$. According to our initial definition of HW operators for discrete phase space, we have $X|q\rangle = |q+1 \mod D\rangle$, which makes the phase space periodic. This periodicity in turn makes the space non-local during evolution. Suppose there is an initial condition with $\psi(0)$ at $q=0$, i.e., a source, whose evolved Wigner function will spread to not only $q=1$ but also to $q=D-1$ due to the mod property of the HW operators. It seems like the time evolution spreads the Wigner function non-locally. However, this apparent non-locality is merely a matter of convention and can be easily addressed by redefining the Wigner function to be defined on a lattice of half-integer separated points $\{0, \frac{1}{2}, 1, \cdots, \frac{D-1}{2}\}$. In this redefined framework, we introduce a new variable Q, where $q = \frac{D}{2} + Q$ in $\mathbb{Z}_D$. This reordering of the phase-point operators is a convenient choice, as it lends a more local appearance to the spread of the Wigner function.

With this new variable Q, the spread of the Wigner function appears more locally defined. For instance, in the expansion, the KW function spreads to the point $Q=\frac{1}{2}$ in the first order, extends up to $Q=1$ in the second order, and so forth. This change in variable allows for a more

intuitive interpretation of the evolution dynamics captured by the Krylov-Wigner function. We can now express the Hamiltonian as a function on the Krylov phase space:

$$\begin{aligned} H(Q,p) &= \frac{1}{D}\,\mathrm{Tr}(HA(Q,p)) \\ &= \frac{1}{D}\sum_{k,\ell=0}^{D-1} \widehat{\delta}_{2Q,k+\ell} e^{\frac{2\pi i}{D}(k-\ell)p} \langle \ell|H|k\rangle \\ &= \frac{1}{D}\sum_{k,\ell=0}^{D-1} \widehat{\delta}_{2Q,k+\ell} e^{\frac{2\pi i}{D}(k-l)p}\,\mathrm{Tr}\left(a_k\delta_{k,\ell} + b_{k+1}\delta_{k+1,\ell} + b_k\delta_{k-1,\ell}\right) \\ &= \frac{1}{D}\left(a_Q + 2b_{Q+\frac{1}{2}}\cos\frac{2\pi p}{D}\right), \end{aligned} \tag{4.7}$$

where we have used (2.17) in the third line for the action of Hamiltonian on the Krylov basis vectors. Now, considering the delta functions in the third line, the non-zero terms are given by:

$$\begin{aligned} H(Q,p) &= \frac{1}{D}\sum_{k,\ell=0}^{D-1} \widehat{\delta}_{2Q,k+\ell} e^{\frac{2\pi i}{D}(k-l)p}\,\mathrm{Tr}\left(a_k\delta_{k,\ell} + b_{k+1}\delta_{k+1,\ell} + b_k\delta_{k-1,\ell}\right) \\ &= \frac{1}{D}\sum_{k}^{D-1}\left(a_k\delta_{2Q,2k} + b_{k+1}e^{-i2\pi p/D}\delta_{2Q,2k+1} + b_k e^{i2\pi p/D}\delta_{2Q,2k-1}\right) \end{aligned} \tag{4.8}$$

Here we have to take into account the fact that there is a modulo D in each of the delta functions, i.e., for the first Kronecker delta, the term is non-zero only when $2k \mod D = 2Q \mod D$. The general solution for k then satisfies $k = Q$. For the second delta function, the term is non-zero only when $(2k+1) \mod D = 2Q \mod D$. No trivial solution is available for this as one can't equalize even and odd numbers. Thus, the solution exists only if one takes into account that both are modulo D. D must be odd, giving rise to the solution $2k+1 = 2Q+D$, or $k = Q + \frac{D-1}{2}$. However, there is another additional restriction on k due to the introduction of a new variable done before to avoid a non-local nature. For $Q + \frac{D+1}{2} > D$, i.e., $Q \geq \frac{D-1}{2}$, $(k+1) \mod D = k - D = Q - \frac{D-1}{2}$. We have for the second Kronecker delta term

$$k+1 = \begin{cases} Q + \frac{D+1}{2} & 0 \leq Q \leq \frac{D-1}{2} - 1 \\ Q - \frac{D-1}{2} & \frac{D-1}{2} \leq Q \leq D-1 \end{cases}$$

For the third delta function, it similarly has non-trivial non-zero solutions for $(2k-1) \mod D = 2Q \mod D$ when $2k-1 = 2Q+D$, or equivalently $k = Q + \frac{D-1}{2}$. The additional restriction is similar to the second Kronecker delta giving rise to the solution

$$k = \begin{cases} Q + \frac{D+1}{2} & 0 \leq Q \leq \frac{D-1}{2} - 1 \\ Q - \frac{D-1}{2} & \frac{D-1}{2} \leq Q \leq D-1 \end{cases}$$

Substituting all these solutions in the Hamiltonian equation, we have

$$H_{(Q,p)} = \frac{1}{D}\begin{cases} a_Q + 2b_{Q+\frac{D+1}{2}}\cos\left(\frac{2\pi}{D}p\right) & 0 \le Q \le \frac{D-1}{2} - 1 \\ a_Q + 2b_{Q-\frac{D-1}{2}}\cos\left(\frac{2\pi}{D}p\right) & \frac{D-1}{2} \le Q \le D-1 \end{cases} \tag{4.9}$$

It is interesting to note that $H_{(Q+D,\ p+D)} = \frac{1}{D}\,\mathrm{Tr}\big(\mathrm{H}A_{(Q+D,\ p+D)}\big) = H_{(Q,p)}$.

4.2 Krylov-Wigner negativity

In discrete phase space, the time evolution of the KW function is given by the discrete version of the Moyal equation (3.42) defined in the Krylov basis. To study the properties of time evolution in the Krylov basis, we first consider the generalized family of Krylov bases which is obtained by multiplying different phases by the individual basis vectors:

$$\mathcal{K} = \{\, e^{i\phi_k}\,|k\rangle \,\}_{k=0}^{D-1} \tag{4.10}$$

where $|k\rangle$ is the k-th basis vector of the Krylov basis. The claim is that for some particular choice of the phases $\{\phi_k\}$, the generalized Krylov basis minimizes the early time growth of Wigner negativity in the large-D limit. The proof developed in [3] is analogous to the one in [2], where it was shown that the Krylov basis minimizes the growth of the spread complexity.

Let's delve into the concept of "minimizing the early time growth of the Wigner negativity." Suppose we have a basis $\mathcal{B}$, and the corresponding Wigner function defined with respect to that basis is denoted by $W_{\mathcal{B}}$. When aiming to minimize the Wigner negativity at $t = 0$, it's evident that we must designate one of the basis vectors as ψ_0. Without loss of generality, let's establish this vector as $|0\rangle_{\mathcal{B}} = |\psi_0\rangle$. With this selection, the logarithm of the Wigner negativity at $t = 0$ vanishes, hence minimizing it.

Now, let's consider the functions:

$$\overline{W}_{\mathcal{B}}^{(m)}(Q,p) = \sum_{n=0}^{m} W_{\mathcal{B}}^{(n)}(Q,p)\frac{t^n}{n!}, \tag{4.11}$$

where $W_{\mathcal{B}}^{(n)} = \frac{d^n W_{\mathcal{B}}}{dt^n}\Big|_{t=0}$. These functions $\overline{W}_{\mathcal{B}}^{(m)}$ represent increasingly accurate Taylor series approximations to the Wigner function in an infinitesimally small neighbourhood of $t = 0$. Now, let's define the set:

$$\mathcal{S}_{\mathcal{B}} = \left\{\mathcal{N}_{\mathcal{B}}^{(0)}, \mathcal{N}_{\mathcal{B}}^{(1)} \cdots, \mathcal{N}_{\mathcal{B}}^{(D-1)}\right\}, \tag{4.12}$$

where

$$\mathcal{N}_{\mathcal{B}}^{(m)} = \sum_{Q,p} |\overline{W}_{\mathcal{B}}^{(m)}(Q,p)|. \tag{4.13}$$

represents the negativity of the mth Taylor series approximation. This is quite similar to the idea behind the proof of the theorem (2.1.1) as discussed in the second chapter. Thus, the idea can be formalized as follows:

Theorem 4.2.1 *For two bases $\mathcal{B}_1$ and $\mathcal{B}_2$, we say that $\mathcal{S}_{\mathcal{B}_1} < \mathcal{S}_{\mathcal{B}_2}$ if there exists some $k < D$ such that $\mathcal{N}_{\mathcal{B}_1}^{(m)} = \mathcal{N}_{\mathcal{B}_2}^{(m)}$ for all $m < k$, and $\mathcal{N}_{\mathcal{B}_1}^{(k)} < \mathcal{N}_{\mathcal{B}_2}^{(k)}$. We say that a basis $\mathcal{B}$ minimizes the growth of the Wigner negativity if for any other basis $\mathcal{B}'$, we have $\mathcal{S}_{\mathcal{B}} \leq \mathcal{S}_{\mathcal{B}'}$.*

Suppose the time evolution occurs in discrete steps with time intervals δt. The goal is to identify a class of bases that minimizes the negativity at each time step. Initially, we aim to minimize negativity at the first time step, then refine this selection to minimize negativity at subsequent steps. To achieve this, we start by considering vectors such as $e^{-i\delta t H}|\psi_0\rangle$ as potential basis elements for the first step. However, before inclusion, each vector must be orthogonalized with respect to ψ_0. Similarly, for subsequent steps, vectors like $e^{-in\delta t H}|\psi_0\rangle$ are considered, but only after orthogonalizing them with respect to the previous basis vectors. In the limit, as δt tends to zero, this approach converges to what is known as the Krylov basis.

Formally, this approach can be understood through the following result, which elucidates the minimization process at the level of the Taylor series approximations in time. By minimizing the early time growth of the Wigner negativity, we aim to achieve the following outcome:

Claim: *In the large-D limit, the basis $\mathcal{B}$ which minimizes the early time growth of Wigner negativity belongs to the class $\mathcal{K}$ of generalized Krylov bases.*

Proof: Since this proof is inspired by the proof in [2], it follows the same nature in the proof, i.e., through induction.

1. Setting up the basis vectors, we assume that the basis vectors $\{|n_{\mathcal{B}}\rangle\}_{n=0}^{d-1}$ must be the generalized Krylov basis form with some particular choice of phases to minimize the first $(d-1)$ elements of $\mathcal{S}_{\mathcal{B}}$. To prove the claim, we need to show that it is required that the dth basis vector coincides with the dth Krylov basis vector, up to a phase, for minimization of the function $\mathcal{N}_{\mathcal{B}}^{(d)}$. So, we consider the initial basis $\mathcal{B}$ such that its first d basis vectors agree

with that of the Krylov basis $\mathcal{K}$, up to phases. We initially don't impose any restrictions on the phases as they are later evaluated by minimizing the elements of $\mathcal{S}_{\mathcal{B}}$.

2. **Step of Induction**: One first need to evaluate the mth time derivative of the Wigner function at $t = 0$, with respect to the chosen set of basis vectors $\mathcal{B}$:

$$\begin{aligned} W_{\mathcal{B}}^{(m)} &= \frac{1}{D}\sum_{k,\ell=0}^{D-1} \widehat{\delta}_{2Q,k+\ell} e^{\frac{2\pi i}{D}(k-\ell)p} \frac{\partial^m}{\partial t^m} \left(\langle k|\psi\rangle \langle\psi|l\rangle\right) \\ &= \frac{1}{D}\sum_{k,\ell=0}^{D-1} \widehat{\delta}_{2Q,k+\ell} e^{\frac{2\pi i}{D}(k-\ell)p} \sum_{n=0}^{m} (-1)^n i^m \frac{m!}{n!(m-n)!} \langle \ell_{\mathcal{B}}|H^n|\psi(0)\rangle \langle\psi(0)|H^{m-n}|k_{\mathcal{B}}\rangle \end{aligned} \tag{4.14}$$

So, the basis vectors of $\mathcal{B}$ are chosen in such a way that $|k_{\mathcal{B}}\rangle = |k_{\mathcal{K}}\rangle$ for $k \leq (d-1)$ and some d. Thus, there are two cases where we need to evaluate and compare $W_{\mathcal{B}}^{(m)}$ and $W_{\mathcal{K}}^{(m)}$:

Case 1: For $m \leq (d-1)$:

In this case, the highest power of Hamiltonian, i.e., H^n, in (4.14) is H^{d-1}. This, when acted on the initial wave function $|\psi(0)\rangle$ produces a linear combination of Krylov basis vectors $|k_{\mathcal{K}}\rangle$ for $k \leq d-1$. Since basis vectors for $\mathcal{B}$ and $\mathcal{K}$ coincide up to the first d ones, the resulting Wigner function of $\mathcal{K}$ basis also matches precisely with that of $\mathcal{B}$:

$$W_{\mathcal{B}}^{(m)} = W_{\mathcal{K}}^{(m)} \tag{4.15}$$

This also implies that the Taylor expansion of the Wigner function around $t = 0$ for both $\mathcal{B}$ and $\mathcal{K}$ agrees up to and including $O(t^{d-1})$ terms.

Case 2: For $m \geq d$:

Let's consider the simplest case of $m = d$ first, where the only difference from the generalized Krylov basis arises from $n = 0$ and $n = d$ terms. The dth derivative of the Wigner function for $m = d$ is given by:

$$W_{\mathcal{B}}^{(d)} = \frac{1}{D}\sum_{k,\ell=0}^{D-1} \widehat{\delta}_{2Q,k+\ell} e^{\frac{2\pi i}{D}(k-\ell)p} \sum_{n=0}^{d} (-1)^n i^d \frac{d!}{n!(d-n)!} \langle \ell_{\mathcal{B}}|H^n|\psi(0)\rangle \langle\psi(0)|H^{d-n}|k_{\mathcal{B}}\rangle \tag{4.16}$$

It can be seen that for $n = 0$ and $n = d$, we have the Hamiltonian term with its highest power as

$$H^d|\psi(0)\rangle = c_d|d_{\mathcal{K}}\rangle + |\chi\rangle \tag{4.17}$$

where $|\chi\rangle$ is some linear combination of the Krylov basis vectors of order lower than d, i.e., $|\chi\rangle = \sum_{n=0}^{d-1} p_n |n_\mathcal{K}\rangle$, and

$$c_d = e^{-i\phi_d} \prod_{n=1}^{d} b_n,$$

where the phase ϕ_d is the phase of the dth basis vector in $\mathcal{K}$ which is yet to be fixed. Now, one need to evaluate the difference between $\langle \ell_\mathcal{K}|H^d|\psi(0)\rangle$ and $\langle \ell_\mathcal{B}|H^d|\psi(0)\rangle$ to compare the Wigner between the two bases.

$$\langle \ell_\mathcal{B}|H^d|\psi(0)\rangle = c_d \langle \ell_\mathcal{B}|d_\mathcal{K}\rangle + \langle \ell_\mathcal{B}|\chi\rangle \tag{4.18}$$

where the second term, $\langle \ell_\mathcal{B}|\chi\rangle$, coincides with $\langle \ell_\mathcal{K}|\chi\rangle$ because $|\chi\rangle$ is a linear combination of Krylov basis vectors up to the first $(d-1)$ vectors, and both $\mathcal{B}$ and $\mathcal{K}$ share the same basis vectors for the first $(d-1)$ terms. Therefore, only the first $(d-1)$ terms, which are identical for both bases, contribute non-zero terms. The difference arises from the term, where it give c_d for $\mathcal{K}$ as it is non-zero for $\ell = d$ as $\langle d_\mathcal{K}|d_\mathcal{K}\rangle$, whereas for $\mathcal{B}$, one finds that $|d_\mathcal{K}\rangle$ is actually distributed to many different orthogonal basis vectors $|\ell_\mathcal{B}\rangle$ for $\ell \geq d$.
The Wigner function for $n = 0$ and $n = d$ becomes

$$\begin{aligned} W_\mathcal{B}^{(d)}(Q,p,n=0,d) &= \frac{1}{D}\sum_{k,\ell=0}^{D-1} \widehat{\delta}_{2Q,k+\ell} e^{\frac{2\pi i}{D}(k-\ell)p} \Big[i^d \langle \ell_\mathcal{B}|\psi(0)\rangle \langle \psi(0)|H^d|k_\mathcal{B}\rangle \\ &\quad + (-i)^d \langle \ell_\mathcal{B}|H^d|\psi(0)\rangle \langle \psi(0)|k_\mathcal{B}\rangle \Big] \\ &= \frac{1}{D}\sum_{k,\ell=0}^{D-1} \widehat{\delta}_{2Q,k+\ell} e^{\frac{2\pi i}{D}(k-\ell)p} \Big[i^d \delta_{\ell_\mathcal{B},0_\mathcal{B}} (c_d^* \langle d_\mathcal{K}|\ell_\mathcal{B}\rangle + \langle \chi|\ell_\mathcal{B}\rangle) \\ &\quad + (-i)^d \delta_{k_\mathcal{B},0_\mathcal{B}} (c_d \langle \ell_\mathcal{B}|d_\mathcal{K}\rangle + \langle \ell_\mathcal{B}|\chi\rangle) \Big]. \end{aligned} \tag{4.19}$$

where the relation (4.18) is used in the second line. Using the delta functions, we can sum over k and ℓ to give us a more compact form:

$$\begin{aligned} W_\mathcal{B}^{(d)}(Q,p,n=0,d) &= \frac{i^d}{D}\sum_{k=0}^{D-1} \widehat{\delta}_{2Q,k} e^{\frac{2\pi i k p}{D}} (c_d^* \langle d_\mathcal{K}|k_\mathcal{B}\rangle + \langle \chi|k_\mathcal{B}\rangle) \\ &\quad + \frac{(-i)^d}{D}\sum_{\ell=0}^{D-1} \widehat{\delta}_{2Q,\ell} e^{-\frac{2\pi i \ell p}{D}} (c_d \langle \ell_\mathcal{B}|d_\mathcal{K}\rangle + \langle \ell_\mathcal{B}|\chi\rangle) \\ &= \frac{1}{D}\sum_{\ell=0}^{D-1} \widehat{\delta}_{2Q,\ell} \left(e^{-\frac{2\pi i}{D}\ell p}(-i)^d \langle \ell_\mathcal{K}|\chi\rangle + e^{\frac{2\pi i}{D}\ell p} i^d \langle \chi|\ell_\mathcal{K}\rangle \right) \\ &\quad + \frac{i^d}{D}\sum_{k=0}^{D-1} \widehat{\delta}_{2Q,k} \left(e^{\frac{2\pi i}{D}kp} c_d^* \langle d_\mathcal{K}|k_\mathcal{B}\rangle + e^{-\frac{2\pi i}{D}kp}(-1)^d c_d \langle k_\mathcal{B}|d_\mathcal{K}\rangle \right). \end{aligned} \tag{4.20}$$

Thus, we get the Wigner function as

$$\begin{aligned}
W_{\mathcal{B}}^{(d)}(Q,p) &= W_{\mathcal{B}}^{(d)}(Q,p,n=0,d) + \sum_{n=1}^{d-1} W_{\mathcal{B}}^{(d)}(Q,p,n) \\
&= \frac{1}{D}\sum_{k,\ell=0}^{D-1} \widehat{\delta}_{2Q,k+\ell} e^{\frac{2\pi i}{D}(k-\ell)p} \sum_{n=1}^{d-1} (-1)^n i^d \frac{d!}{n!(d-n)!} \langle \ell_{\mathcal{K}}|H^n|\psi(0)\rangle\langle\psi(0)|H^{d-n}|k_{\mathcal{K}}\rangle \\
&+ \frac{1}{D}\sum_{\ell=0}^{D-1} \widehat{\delta}_{2Q,\ell} \left(e^{-\frac{2\pi i}{D}\ell p}(-i)^d \langle \ell_{\mathcal{K}}|\chi\rangle + e^{\frac{2\pi i}{D}\ell p} i^d \langle \chi|\ell_{\mathcal{K}}\rangle \right) \\
&+ \frac{i^d}{D}\sum_{k=0}^{D-1} \widehat{\delta}_{2Q,k} \left(e^{\frac{2\pi i}{D}kp} c_d^* \langle d_{\mathcal{K}}|k_{\mathcal{B}}\rangle + e^{-\frac{2\pi i}{D}kp}(-1)^d c_d \langle k_{\mathcal{B}}|d_{\mathcal{K}}\rangle \right).
\end{aligned} \tag{4.21}$$

To compare the Wigner function of $\mathcal{B}$ with that of $\mathcal{K}$, one needs to evaluate $W_{\mathcal{K}}^{(d)}(Q,p,n=0,d)$ as it takes the same form for the rest of the values of n:

$$\begin{aligned}
W_{\mathcal{K}}^{(d)}(Q,p,n=0,d) = \frac{i^d}{D}\sum_{k=0}^{D-1} \widehat{\delta}_{2Q,k} e^{\frac{2\pi i k p}{D}} \left(c_d^* \langle d_{\mathcal{K}}|k_{\mathcal{K}}\rangle + \langle \chi|k_{\mathcal{K}}\rangle \right) \\
+ \frac{(-i)^d}{D}\sum_{\ell=0}^{D-1} \widehat{\delta}_{2Q,\ell} e^{-\frac{2\pi i \ell p}{D}} \left(c_d \langle \ell_{\mathcal{K}}|d_{\mathcal{K}}\rangle + \langle \ell_{\mathcal{K}}|\chi\rangle \right),
\end{aligned} \tag{4.22}$$

Here, it can be observed that the terms with coefficient c_d and c_d^* are non-zero only for $k = d$ and $\ell = d$. Thus, quantity can be divided into two quantities: the first term containing the sum till $d-1$ terms and the second containing the dth term. The first term is synonymous with the results of $W_{\mathcal{B}}^{(d)}(Q,p,n=0,d)$ if the same treatment is applied there. So, equation (4.23) becomes:

$$\begin{aligned}
W_{\mathcal{K}}^{(d)}(Q,p,n=0,d) &= \frac{i^d}{D}\sum_{k=0}^{d-1} \widehat{\delta}_{2Q,k} e^{\frac{2\pi i k p}{D}} \langle \chi|k_{\mathcal{K}}\rangle + \frac{(-i)^d}{D}\sum_{\ell=0}^{d-1} \widehat{\delta}_{2Q,\ell} e^{-\frac{2\pi i \ell p}{D}} \langle \ell_{\mathcal{K}}|\chi\rangle \\
&+ \frac{i^d}{D}\widehat{\delta}_{2Q,d} \left(c_d^* e^{\frac{2\pi i d p}{D}} + (-1)^d c_d e^{-\frac{2\pi i d p}{D}} \right) \\
&= \frac{i^d}{D}\sum_{k=0}^{d-1} \widehat{\delta}_{2Q,k} e^{\frac{2\pi i k p}{D}} \langle \chi|k_{\mathcal{K}}\rangle + \frac{(-i)^d}{D}\sum_{\ell=0}^{d-1} \widehat{\delta}_{2Q,\ell} e^{-\frac{2\pi i \ell p}{D}} \langle \ell_{\mathcal{K}}|\chi\rangle \\
&+ \frac{i^d}{D}\sum_{k=d}^{D-1} \widehat{\delta}_{2Q,k} \left(c_d^* e^{\frac{2\pi i d p}{D}} \langle d_{\mathcal{K}}|k_{\mathcal{B}}\rangle + (-1)^d c_d e^{-\frac{2\pi i d p}{D}} \langle k_{\mathcal{B}}|d_{\mathcal{K}}\rangle \right) \\
&- \frac{i^d}{D}\sum_{k=d}^{D-1} \widehat{\delta}_{2Q,k} \left(c_d^* e^{\frac{2\pi i d p}{D}} \left(\langle d_{\mathcal{K}}|k_{\mathcal{B}}\rangle - \delta_{k,d} \right) + (-1)^d c_d e^{-\frac{2\pi i d p}{D}} \left(\langle k_{\mathcal{B}}|d_{\mathcal{K}}\rangle - \delta_{k,d} \right) \right) \\
W_{\mathcal{K}}^{(d)}(Q,p,n=0,d) &= W_{\mathcal{B}}^{(d)}(Q,p,n=0,d) \\
&- \frac{i^d}{D}\sum_{k=d}^{D-1} \widehat{\delta}_{2Q,k} \left(c_d^* e^{\frac{2\pi i d p}{D}} \left(\langle d_{\mathcal{K}}|k_{\mathcal{B}}\rangle - \delta_{k,d} \right) + (-1)^d c_d e^{-\frac{2\pi i d p}{D}} \left(\langle k_{\mathcal{B}}|d_{\mathcal{K}}\rangle - \delta_{k,d} \right) \right)
\end{aligned} \tag{4.23}$$

Since it is already established that $\sum_{n=1}^{d-1} W_{\mathcal{B}}^{(d)}(Q,p,n) = \sum_{n=1}^{d-1} W_{\mathcal{K}}^{(d)}(Q,p,n)$, equation (4.21) can be re-written using (4.23) as:

$$\begin{aligned} W_{\mathcal{B}}^{(d)}(Q,p) = W_{\mathcal{K}}^{(d)}(Q,p) + \frac{i^d}{D}\sum_{k=d}^{D-1} \widehat{\delta}_{2Q,k} \Big[c_d^* e^{\frac{2\pi i}{D}kp}(\langle d_{\mathcal{K}}|k_{\mathcal{B}}\rangle - \delta_{k,d}) \\ + c_d e^{-\frac{2\pi i}{D}kp}(-1)^d(\langle k_{\mathcal{B}}|d_{\mathcal{K}}\rangle - \delta_{k,d})\Big] \end{aligned} \tag{4.24}$$

Now, ϕ_d is temporarily fixed by ensuring that $\langle d_{\mathcal{B}}|d_{\mathcal{K}}\rangle$ is a real number within the range $[0,1]$. This selects a specific member from the set of generalized Krylov bases. It is aimed to be shown that this basis already exhibits lower negativity compared to $\mathcal{B}$, and subsequently, minimizing over ϕ_d will further reduce the negativity. The whole point of the proof is to show that sum negativity follows $\mathrm{sn}(W_{\mathcal{B}}^{(d)}) \geq \mathrm{sn}(W_{\mathcal{K}}^{(d)})$ for all choices of $\mathcal{B}$. Let us denote:

$$\langle k_{\mathcal{B}}|d_{\mathcal{K}}\rangle = \delta_{d,k} + \alpha_k, \;\; \cdots \;\; (k \geq d) \tag{4.25}$$

where $\alpha_d \in \mathbb{R}$ and $-1 \leq \alpha_d \leq 0$ (by restricting ϕ_d), and

$$(1+\alpha_d)^2 + \sum_{k=d+1}^{D-1} |\alpha_k|^2 = 1. \tag{4.26}$$

Here, the identity of α_k's can be derived from the fact that $|d_{\mathcal{K}}\rangle$ is distributed among numerous basis vectors in $\mathcal{B}$. So,

$$\sum_{k=d}^{D-1} |\langle k_{\mathcal{B}}|d_{\mathcal{K}}\rangle|^2 = 1$$

$$(1+\alpha_d)^2 + \sum_{k=d+1}^{D-1} |\langle k_{\mathcal{B}}|d_{\mathcal{K}}\rangle|^2 = (1+\alpha_d)^2 + \sum_{k=d+1}^{D-1} |\alpha_k|^2 = 1$$

Let $\alpha_k = |\alpha_k|e^{i\theta_k}$, $c_d = |c_d|e^{-i\phi_d}$ and $\Theta_{2Q\geq d}$ be a step function which is one only when $2Q \geq d$ and zero otherwise. Equation (4.24) can thus be represented as:

$$W_{\mathcal{B}}^{(d)}(Q,p) = \begin{cases} W_{\mathcal{K}}^{(d)}(Q,p) + \dfrac{2(-1)^{\frac{d}{2}}}{D}|c_d||\alpha_{2Q}|\Theta_{2Q\geq d}\cos\left(\dfrac{2\pi(2Q)p}{D} + \theta_{2Q} + \phi_d\right) & \cdots (d \text{ even}) \\ W_{\mathcal{K}}^{(d)}(Q,p) + \dfrac{2(-1)^{\frac{d-1}{2}}}{D}|c_d||\alpha_{2Q}|\Theta_{2Q\geq d}\sin\left(\dfrac{2\pi(2Q)p}{D} + \theta_{2Q} + \phi_d\right) & \cdots (d \text{ odd}), \end{cases} \tag{4.27}$$

The Wigner negativity till $(d-1)$th order is the same both bases $\mathcal{B}$ and $\mathcal{K}$, whereas the negativity at dth order is given by

$$\mathcal{N}^{(d)} = \sum_{Q,p} |\overline{W}_{\mathcal{B}}^{(d)}(Q,p)|. \tag{4.28}$$

For terms up to $O(t^{d-1})$, i.e. for $2Q < d$, the Wigner function in this region is exactly equal to the Wigner function in generalized Krylov basis:

$$\overline{W}_{\mathcal{B}}^{(d)}(Q,p) = \overline{W}_{\mathcal{K}}^{(d)}(Q,p), \quad \forall \ 2Q < d. \tag{4.29}$$

So, the difference arises from the region with $2Q \geq d$, which can be determined from the comparison of $\sum_{2Q\geq d,p} \overline{W}_{\mathcal{B}}^{(d)}(Q,p)$ with $\sum_{2Q\geq d,p} \overline{W}_{\mathcal{K}}^{(d)}(Q,p)$. The proof is given in [3] for the case where d is even. Let's first consider the case for odd d, where equation (4.27) becomes:

$$W_{\mathcal{B}}^{(d)}(d/2,p) = W_{\mathcal{K}}^{(d)}(d/2,p) + \frac{2(-1)^{\frac{d-1}{2}}}{D}|c_d||\alpha_{2Q}|\Theta_{2Q\geq d}\sin\left(\frac{2\pi(2Q)p}{D} + \theta_{2Q} + \phi_d\right) \tag{4.30}$$

For $2Q = d$, the second term in the equation (4.30) becomes

$$-\frac{2i^{d+1}}{D}|c_d||\alpha_d|\sin\left(\frac{2\pi pd}{D} + \phi_d\right)$$

whereas for $2Q > d$, the second term becomes

$$\frac{2i^{d+1}}{D}|c_d||\alpha_{2Q}|\sin\left(\frac{4\pi Qp}{D} + \phi_d + \theta_{2Q}\right)$$

To compare the Wigner negativity for the two bases, we want to compare $\sum_{2Q\geq d,p}\left|W_{\mathcal{B}}^{(d)}(Q,p)\right|$ and $\sum_{2Q\geq d,p}\left|W_{\mathcal{K}}^{(d)}(Q,p)\right|$. Applying triangle inequality to the equation (4.30), one gets:

$$\left|W_{\mathcal{K}}^{(d)}(Q,p)\right| \leq \left|W_{\mathcal{B}}^{(d)}(Q,p)\right| + \frac{2}{D}|c_d||\alpha_{2Q}|\left|\sin\left(\frac{2\pi(2Q)p}{D} + \theta_{2Q} + \phi_d\right)\right|. \tag{4.31}$$

Summing over all Q for $2Q \geq d$, we get

$$\sum_{Q\geq d/2}\left|W_{\mathcal{K}}^{(d)}(Q,p)\right| \leq \sum_{Q\geq d/2}\left|W_{\mathcal{B}}^{(d)}(Q,p)\right| + \frac{2}{D}|c_d|\sum_{Q\geq d/2}|\alpha_{2Q}|\left|\sin\left(\frac{2\pi(2Q)p}{D} + \theta_{2Q} + \phi_d\right)\right|$$

Again using triangle inequality $|a-b| \geq |a| - |b|$ for the second term

$$\begin{aligned}\sum_{Q\geq d/2}\left|W_{\mathcal{K}}^{(d)}(Q,p)\right| \leq \sum_{Q\geq d/2}\left|W_{\mathcal{B}}^{(d)}(x,p)\right| + \frac{2}{D}|c_d|\Big\{|\alpha_d|\left|\sin\left(\frac{2\pi dp}{D} + \phi_d\right)\right| \\ - \sum_{Q>d/2}|\alpha_{2Q}|\left|\sin\left(\frac{4\pi Qp}{D} + \theta_{2Q} + \phi_d\right)\right|\Big\}.\end{aligned} \tag{4.32}$$

Now, summing over all discrete momentum points p up to $D-1$, the sum can be converted into an integral equation for the large D limit. The differentiating term can be approximated by integrals, which gives

$$\sum_{p,Q\geq d/2}|W_{\mathcal{K}}^{(d)}(Q,p)| \leq \sum_{p,Q\geq d/2}|W_{\mathcal{B}}^{(d)}(Q,p)| + \frac{4|c_d|}{\pi}\left(d|\alpha_d| - \sum_{k>d}k|\alpha_k|\right). \tag{4.33}$$

The goal now is to show that $d|\alpha_d| \leq \sum_{k>d} k|\alpha_k|$. Using equation (4.26), we have

$$(1+\alpha_d)^2 + \sum_{k>d} |\alpha_k|^2 = 1$$

$$-2|\alpha_d| + |\alpha_d|^2 + \sum_{k>d} |\alpha_k|^2 = 0.$$

Since $|\alpha_d|$ and $|\alpha_k|$'s are all positive numbers less than 1, we have $|\alpha_d| > |\alpha_d|^2$ and $\sum_{k>d} |\alpha_k| > \sum_{k>d} |\alpha_k|^2$. The above relation becomes:

$$\begin{aligned} -|\alpha_d| + \sum_{k>d} |\alpha_k|^2 &= |\alpha_d| - |\alpha_d|^2 \\ -|\alpha_d| + \sum_{k>d} |\alpha_k|^2 &\geq 0 \\ -|\alpha_d| + \sum_{k>d} |\alpha_k| &\geq 0 \\ \left(\text{Using} \sum_{k>d} |\alpha_k| > \sum_{k>d} |\alpha_k|^2\right) & \\ \sum_{k>d} |\alpha_k| &\geq |\alpha_d| \end{aligned} \tag{4.34}$$

It immediately follows from the above relation that

$$d|\alpha_d| \leq \sum_{k>d} k|\alpha_k|. \tag{4.35}$$

as each k is greater than d.

Hence, it is hereby proved that for any given basis $\mathcal{B}$, we can adjust the phase of the dth generalized Krylov basis vector to reduce its negativity compared to $\mathcal{B}$. By minimizing the negativity over the choice of this phase for the dth Krylov basis vector, we ensure the existence of a generalized Krylov basis that minimizes the negativity up to this order.

Therefore, selecting appropriately phased generalized Krylov bases effectively mitigates the early growth of Wigner negativity in the large D limit. Consequently, when aiming to simulate quantum dynamics on a classical computer, the Krylov basis, with carefully chosen phases, emerges as a promising option for the computational basis. However, it's important to note that we haven't provided a specific algorithm here for efficiently simulating time evolution in the Krylov basis. Nevertheless, our findings lend credence to the notion that the Krylov basis possesses unique attributes conducive to classical simulation of quantum dynamics.

Furthermore, the Krylov basis holds intriguing potential as a "dual gravitational basis" for strongly coupled quantum systems. Equation (4.9) serves as a natural analog of the gravitational Hamiltonian. Remarkably, in the DSSYK model, the dual "gravitational" description aligns with the chord-length basis, which precisely coincides with the Krylov basis. This alignment suggests that the gravitational variables may correspond to a basis selection optimizing classical simulation efficiency for quantum dynamics.

4.3 Growth of KW negativity

Having demonstrated that generalized Krylov bases effectively minimize the initial growth of discrete Wigner negativity across all basis selections, one naturally ponders the behaviour of negativity growth in various scenarios concerning the KW function. Ideally, one would like to apply this framework to the most natural models like the DSSYK model or the SSS matrix model, but due to time constraints, it is more convenient to consider Gaussian random matrix theory. The Gaussian Unitary Ensemble (GUE) is regarded in [3], so we'll consider the case for the Gaussian Orthogonal Ensemble (GOE). The Krylov basis considered below has no phases attached to them. It's intriguing to explore and prove what exactly the phases that optimize the growth of the KW function turn out to be for each individual basis vector. It is interesting to note that the expected result turns out to be zero for each individual basis vector.

4.3.1 KW function for GOE

We first generate a working coordinate basis, where one of the basis vectors is declared as $|0\rangle$ coinciding with the initial state ψ_0. The next requirement is the Hamiltonian to study the time evolution of all the quantities as well as the basis vectors themselves. In our coordinate basis, the Hamiltonian is taken as a $D \times D$ matrix from the Gaussian Orthogonal Ensemble (GOE). The GOE has the probability distribution $p(H)$ over the space of Hermitian matrices:

$$p(H) = \frac{1}{Z_{GOE}} e^{-\frac{D}{4}\,\mathrm{Tr}(H^2)} \tag{4.36}$$

where $Z_{GOE} = (2)^{-1/2}(2\pi)^{-\frac{D(D+1)}{4}}$ is the partition function, normalizing the probability distribution. In these conventions, the variance of each off-diagonal matrix entry for all ensembles is fixed to $\sigma^2 = 1/D$.

We proceed by constructing the Krylov basis starting from the state $|0\rangle$, and then iteratively

applying the Hamiltonian operator while orthogonally normalizing the basis using the Gram-Schmidt process. Once we have established a Krylov basis spanning the Hilbert space, we proceed to construct the KW function and evaluate its negativity over time. The negativity is defined by:

$$\mathcal{N}(t) = \sum_{Q,p} \left| W_{\psi(t)}(Q,p) \right| \tag{4.37}$$

where $|\psi(t)\rangle = e^{-iHt} |\psi_0\rangle$.

4.3.2 Analysis

The result is similar to the results cited by O. Parrikar et. al in [3]. This is expected as GUE and GOE exhibit similar level spacing distributions between adjacent eigenvalues of the random matrices.

The negativity of the Wigner function is numerically calculated and plotted against re-scaled time $t/\sqrt{D}$ for different values of D. The trend is more decipherable for higher values of D. We have obtained the plots for $D = 51, 101, 151$ and 201.

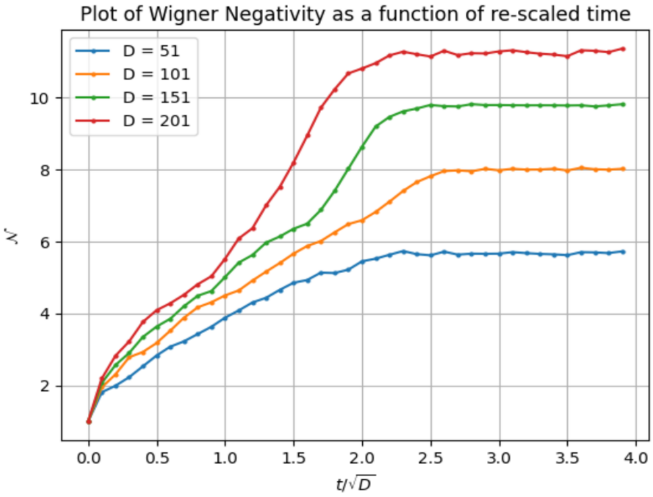

Figure 4.1. Negativity of the Wigner function $\mathcal{N}$ as a function of the e-scaled time $\frac{t}{\sqrt{D}}$ for a randomly chosen Hamiltonian from the GOE for various values of D.

It can be clearly observed for higher D, e.g. for $D = 151$ and $D = 201$, that the un-normalized numerical plots can be broadly divided into three distinct phases:

(i) **Spreading phase**: This is the first phase with the relatively slow and gradual growth of Wigner negativity from an early time.

(ii) **Ramp or Ascent phase**: The Wigner negativity experiences a rapid increase forming a sharp ramp or steep ascent phase. The ascent follows a nearly linear slope at time $t \sim O(\sqrt{D})$. Numerically, for $D = 201$, the slope turns out to be about ~ 6.6 which is of the order of $O(\sqrt{D})$.

(iii) **Saturation phase**: At late times, the Wigner negativity saturates to a plateau with the saturation value increasing for higher D values.

One can also normalize the Wigner negativity to be independent of the dimensional parameter D. It turns out that the normalization factor of GOE is the same as in the GUE distribution [3], i.e., $1/\sqrt{D}$. The y-axis is now re-calibrated for the normalized Wigner negativity $\mathcal{N}/\sqrt{D}$ and re-plotted for the various values of D:

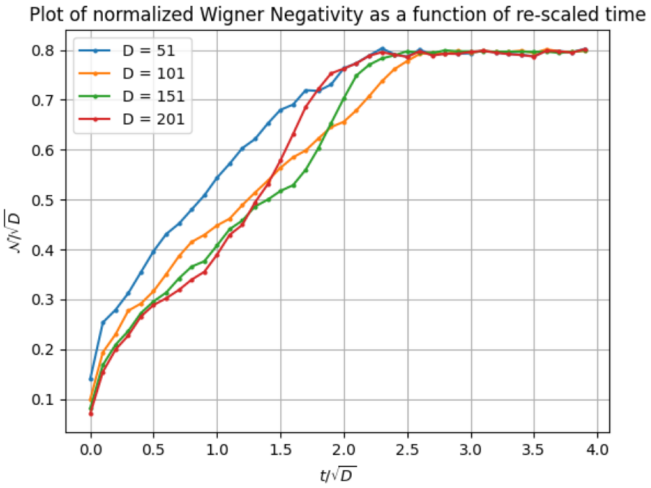

Figure 4.2. Normalized Negativity of the Wigner function $\mathcal{N}/\sqrt{D}$ as a function of the re-scaled time $\frac{t}{\sqrt{D}}$ for a randomly chosen Hamiltonian from the GOE for various values of D.

It can be observed that the normalized Wigner negativity saturates at approximately $\mathcal{N}_s \sim 0.8\sqrt{D}$ at late times. The plot can be explained by studying the evolution of the Krylov-Wigner function in phase space:

- At $t = 0$, the Wigner function is initially localized as a line parallel to the momentum axis at $Q = 0$ as the initial function itself is $|0\rangle$. As the wavefunction starts to evolve, at very early times, the Wigner function spread uniformly over the momentum direction as can be observed from (4.6):

$$W(0, Q, p) = \frac{1}{D}\delta_{Q,0}. \tag{4.38}$$

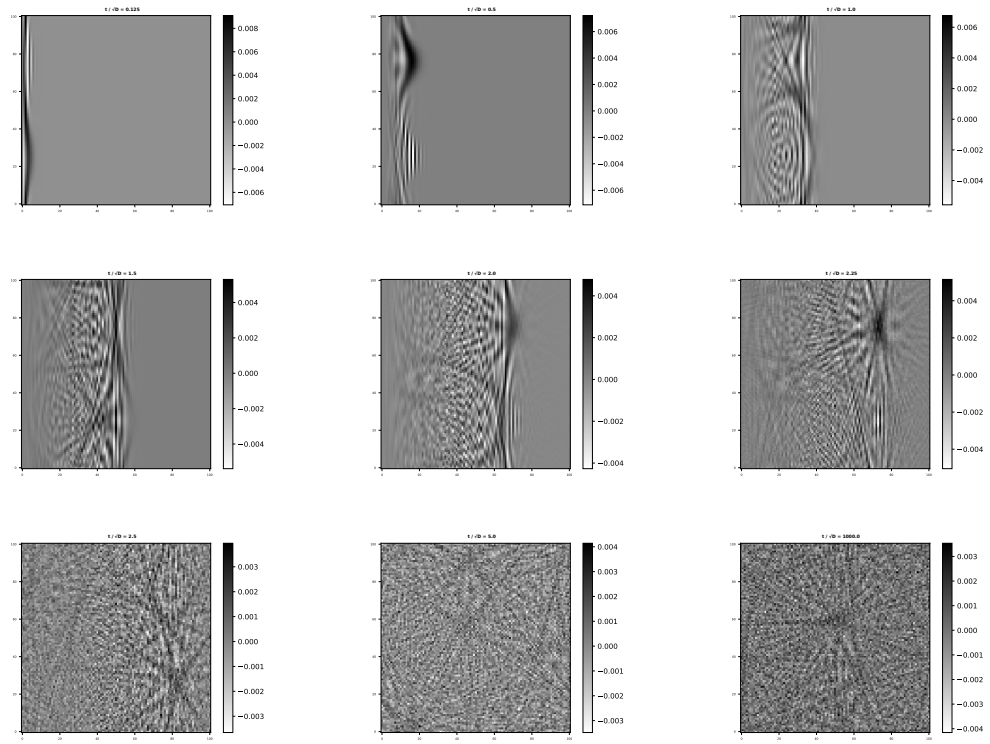

Figure 4.3. Density plots of the Krylov-Wigner function in phase space for $D = 101$ for various values of time corresponding to $\frac{t}{\sqrt{D}} = (0.125, 0.5, 1, 1.5, 2, 2.25, 2.5, 5, 1000)$. Governed by GUE matrix theory. Cited from: *R. Basu, O. Parrikar et. al* [5][3]

- As time increases, the Wigner function spreads slowly in the phase space, as the later terms come into play. In this spread phase, the Wigner negativity grows gradually with time. It is characteristic of the Krylov basis that the growth of Wigner negativity is slower than any other computational basis possible. At early times, the Krylov-Wigner function is localized, so the sine term is small, leading to the gradual spread.
- As time progresses, the leading term is the linear term in time. The Krylov-Wigner function delocalizes, the sine term becomes larger, and the rapid ramp in negativity occurs. Eventually, the Krylov-Wigner function saturates the phase space and the negativity plateaus.
- In figure (4.3.), the time evolution of the Wigner function is depicted over the phase space under the GUE Hamiltonian for $D = 101$. This is similar to the one evolved under the GOE Hamiltonian. When we talk about the Wigner negativity or sum negativity, we refer to the values depicted by the white areas in the plot (4.3.).

Initially, with the Wigner function concentrated around $Q = 0$, there's minimal negativity due to the completely Gaussian-like initial state. As the wavefunction expands to higher Q values, negative values for Wigner functions emerge over various phase points (both the newly acquired Q values and the old ones), gradually increasing in proportion to the positive values of Wigner functions over phase points. Since the Wigner negativity counts the sum of only negative Wigner functions, essentially all the positive Wigner functions are set to zero in the sum. As the wavefunction evolves and occupies higher and higher Q values, the Wigner function at phase points with lower Q values begins to disperse, i.e., the negative and positive values of the Wigner function begin to disperse uniformly across these phase points. Meanwhile, the rapidly evolving wavefunction at higher Q values generates new phase points with negative Wigner function values. Eventually, the dispersion accelerates as the Wigner function spreads across the entire phase space. This leads to a rapid growth in the Wigner negativity, i.e., it acquires linear growth behaviour with a steep slope. The negativity reaches a near-saturation level, typically at around $0.8\sqrt{D}$ for GOE as well as GUE Hamiltonians, as we reach higher time.

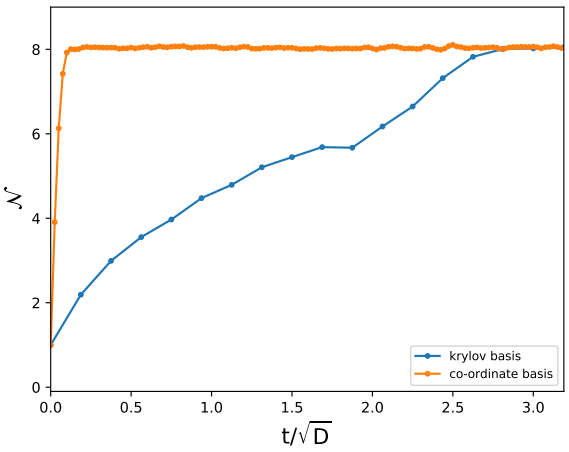

Figure 4.4. The negativity of the Wigner function with respect to the coordinate basis in comparison with that of the Krylov-Wigner function for $D = 101$.
Cited from: *R. Basu, O. Parrikar et. al* [5][3]

Compared to any other generic basis, the growth of the Wigner negativity is slowest in the Krylov basis as already discussed. This behaviour can be clearly observed in fig (4.4.), where the growth of negativity of the Wigner function in the Krylov basis is compared with respect

to that in the coordinate basis. In the Krylov basis, the negativity increases gradually over time reaching saturation, whereas in the coordinate basis, the negativity rises at $t = 0$ itself, following a steep slope of $O(\sqrt{D})$ and saturates within a time of $O(1)$. This is the expected behaviour of all generic bases. In the case of the KW function, the slope can be calculated from the expanded expression of the Krylov-Wigner function (4.6). Using $H|0\rangle = a_0|0\rangle + b_1|1\rangle$ for first order evolution, we get

$$W(t,Q,p) = \frac{1}{D}\delta_{2Q,0} - \frac{2tb_1}{D}\sin\left(\frac{2\pi p}{D}\right)\delta_{2Q,1} + O(t^2). \tag{4.39}$$

So, at linear time, the Wigner negativity contains the sum of only two Q values, i.e. $Q = 0$ and $Q = 1/2$:

$$\begin{aligned}\mathcal{N} &= \frac{1}{D}\left(\delta_{0,0} + \delta_{1,0}\right) + \frac{2tb_1}{D}\sum_{p=0}^{D-1}|sin|\left(\frac{2\pi p}{D}\right)\left(\delta_{0,1} + \delta_{1,1}\right) \\ &= \frac{1}{D}\delta_{2Q,0} - \frac{2tb_1}{D}\sin\left(\frac{2\pi p}{D}\right)\delta_{2Q,1} + O(t^2).\end{aligned} \tag{4.40}$$

In large D limit, this sum can be converted in an integral over p:

$$\mathcal{N} = 1 + \frac{2t}{2\pi}b_1\int_0^{2\pi} d\theta|\sin(\theta)| = 1 + \frac{4t}{\pi}b_1 + O(t^2). \tag{4.41}$$

Thus, we have a linear dependence with time with a slope proportional to b_1. The expectation value of $\overline{b_1}$ depends on the chosen distribution. It turns out to be $O(1)$ in the case of GUE [3], which with observation of the fact that GOE behaves nearly similar to GUE, the value should be nearly of the same order. It can be also observed that as $t/\sqrt{D}$ becomes $O(1)$, the Wigner function spreads nearly over the entire phase space. The slope of the Wigner negativity here is $O(\sqrt{D})$, which we have defined as the ramp phase.

Hence, our observations are shown to match with those of [3] as to how the Wigner negativity evolves over time.

Chapter 5

Conclusions and Future Work

In this thesis, we investigated the notion of Krylov complexity within the framework of quantum chaos, based on the work of V. Balasubramaniam [**Balasubramaniam**]. Additionally, we examined the Wigner function in the context of discrete phase space, following the approach outlined by Wootters [**Wootters**]. Our study focused on the concept of negativity in the discrete Wigner function and its connection to the stabilizer and non-stabilizer states in quantum computation. We quantified this relationship through the use of *magic states*, demonstrating that the sum negativity of the discrete Wigner function exhibits properties akin to those of a magic state [**Veitch**]. Combining these concepts of Krylov complexity and Negativity of discrete Wigner function, we introduced the Krylov-Wigner function which is the discrete Wigner function with respect to a specific choice of basis, i.e., the Krylov basis. With an appropriate choice of basis, it is shown that the KW function minimizes the growth of negativity of the Wigner function for early time for large D limit in quantum systems [5]. The KW negativity behaves in a particular fashion, where it grows till a time exponential in $\log D$, then saturates at exponentially large time values.

The framework of the KW function is then applied to the Gaussian Orthogonal Ensemble (GOE) and the results are compared with that of GUE. Since the ideal application of the developed framework will be on natural models like the DSSYK model or the SSS matrix model, the future direction for this work will be the investigation of the said function in the SSS matrix model which is currently underway. Additionally, we have only discussed the case of pure state at zero β (infinite temperature) as opposed to the general case of finite β (finite temperatures). This can be done using the discussed Thermo-Field Double (TFD) states and the temperature dependence of the KW negativity can thus be studied.

It is interesting to note that the Krylov basis appears naturally in the dual gravitational description as the eigenstates of the length operator of the bulk wormhole, in the context of the DSSYK model. The negativity of the KW function is a measure of the "quantum-ness" in a quantum state. The fact that Krylov basis minimizes the early-time growth of the Wigner

negativity, advocates the claim that it is ideally suited for a dual semi-classical description of chaotic quantum systems. The most important aspect of chaos is ergodicity, i.e., the Wigner function will spread out and eventually cover the phase space uniformly, indicating that the system's state has explored all possible configurations. Due to this, the Krylov basis can encode the full spectrum of states and dynamics of the boundary CFT, making it an effective representation of CFT. The AdS/CFT correspondence often relates chaotic behaviour in the boundary CFT to the dynamics of black holes and other gravitational phenomena in the bulk. A Krylov basis that captures this chaos and complexity through ergodic behaviour is likely to map well onto the gravitational degrees of freedom in the bulk AdS space. These implications supported the proposal of a new computational principle for the emergence of spacetime and gravity [5]:

> *The gravitational variables correspond to a choice of basis which makes classical implementation of quantum computation as efficient as possible.*

There are several problems that need to be addressed in order to make this claim concrete. The concept of the Krylov basis being the dual description is shown to work for discrete phase space at finite D. For concrete application to continuum gravity, one needs to show that it also applies to large D limit of the DSSYK model. One would want a more general treatment of the dimensionality D, rather than the case of prime D which we have considered. This would also help in the generalization of the theory to large D limit. Another future prospect of this work is developing models of quantum circuits and study the relationship between Wigner negativity and magic monotone channels further.

Bibliography

[1] V. Balasubramanian, J.M. Magan, and Q. Wu. "Tridiagonalizing random matrices". In: *Phys. Rev. D* 107.126001 (2023). DOI: 10.1103/PhysRevD.107.126001. arXiv: 2208.08452 [hep-th]. URL: https://arxiv.org/abs/2208.08452.

[2] V. Balasubramanian et al. "Quantum chaos and the complexity of spread of states". In: *Phys. Rev. D* 106.046007 (2022). DOI: 10.1103/PhysRevD.106.046007. arXiv: 2202.06957 [hep-th]. URL: https://arxiv.org/abs/2202.06957.

[3] R. Basu et al. "Complexity Growth and the Krylov-Wigner function". In: *arXiv: Prepared for submission to JHEP* (2024). arXiv: 2402.13694 [hep-th]. URL: https://arxiv.org/abs/2402.13694.

[4] W.B. Case. "Wigner functions and Weyl transforms for pedestrians". In: *Am. J. Phys.* 76.10 (2008), pp. 937–946. DOI: 10.1119/1.2957889.

[5] V. Veitch et al. "The resource theory of stabilizer quantum computation". In: *New Journal of Physics* 16.013009 (2014). DOI: 10.1088/1367-2630/16/1/013009.

[6] X. Wang, M.M. Wilde, and Y. Su. "Quantifying the magic of quantum channels". In: *New Journal of Physics* 21.103002 (2019). DOI: 10.1088/1367-2630/ab451d.

[7] W.K. Wootters. "A wigner-function formulation of finite-state quantum mechanics". In: *Annals of Physics* 176 (1987), pp. 1–21. DOI: 10.1016/0003-4916(87)90176-X.